Investigating the micromechanics of interfaces shearing against granular material

By

A. D. Campbell (G)

Fourth year undergraduate project

In Group D (2013-2014)

Technical abstract

There is so much to learn about the soil-structure interface and the effect of interface roughness. According to recent research, the widely accepted assumption that rough interfaces produce higher interface friction than smooth interfaces may not be true. Further research is needed in order to understand fully the micromechanics of the soil-structure interface. The effect of roughness has serious implications for the shear behaviour of deepwater hot oil pipelines and the amount of soil participating in the shearing.

This project investigates the movement of grains and the stresses induced around the soil-structure interface when a sample of granular material is sheared by interfaces of different roughnesses. Photoelastic effects and Particle Image Velocimetry (PIV) are used on a vertical array of several thousand discs to simulate the soil-structure interface. Acrylic discs are sheared and PIV is used to produce a vector plot of the particle movements around the soil-structure interface. Polyurethane discs are sheared and a circular polarising polariscope is used to view the stress paths around the soil-structure interface. The results of these two sets of experiments are compared and links between the results are investigated.

The experiments produce three key results relating to the height of the zone of influence. The zone of influence is taken as the area of particles where displacement or stresses are significantly affected by the movement of the interface. For the array of acrylic discs, the height of the zone of influence is taken as the height below which there is significant movement, which can be deduced form the vector plot, produced by PIV. For the polyurethane discs, the height of the zone of influence is taken as the height below which there is significant stress in the particles, which can clearly be deduced from the images of the array under shearing.

The three key results are as follows:

- The height of the zone of influence is the same for the acrylic and polyurethane arrays
- The height of the zone of influence increases with the relative roughness
- Unexpectedly, the height of the zone of influence decreases linearly with the angle of attack of the interface.

In terms of interface simulation, the larger the relative roughness of an interface, the rougher the surface that it simulates. The results of this project therefore suggest that the motion of a rougher surface shearing an array of soil will engage a larger volume of soil than a smoother

surface will and the soil resists the motion of the shearing surface with greater participation when the surface is rough than when it is smooth.

This project, therefore, provides crucial research and findings to aid the design and construction of oil pipelines. By applying these findings to the case of oil pipelines resting on the sea bed, if the pipelines are covered with a rough coating they will feel a greater resistance to motion from the soil beneath them than if they had a smooth coating.

Contents

1 Introduction 1

1.1 Motivation for the project 1

1.2 Previous research 1

1.3 Focus of the research and report outline 3

2 Theory and design of experiment **5**

2.1 Aims of the investigation 5

2.2 Particle Image Velocimetry (PIV) 6

2.3 Photoelasticity 10

2.4 Design of the experiments 13

2.5 Hypotheses 14

3 Apparatus and method **15**

3.1 Apparatus components 15

3.2 Issues overcome 19

4 Results **22**

4.1 Acrylic discs 22

4.2 Polyurethane discs 29

5 Discussion **33**

5.1 Testing the hypotheses 33

5.2 Further discussion 39

6 Conclusions **41**

6.1 Key results 41

6.2 Reservations and limitations 41

6.3 Implications of the key results 41

6.4 Ideas for future work 41

Acknowledgements **43**

References **43**

Appendices

A Risk assessment retrospective **45**

Chapter 1: Introduction

1.1 Motivation for the project

Engineers desire to know more about grain movement around the soil-structure interface, which is a key area for many scenarios including interface shear behaviour for deepwater hot oil pipelines.[1] The widely-accepted assumption that rough interfaces produce higher interface friction than smooth interfaces has been observed not necessarily to hold true for deep ocean, highly structured soft clays.[2]

The interaction between deepwater hot oil pipelines and the soil on which they rest is a fundamental issue. The effect that the roughness of an interface may have on the movement and stress distribution in the soil has great applications in this area and the results may lead to changes in the ways in which the pipelines are designed and coated. It is desirable to minimise the movement of soil and the stresses induced in the soil matrix as a result of the pipeline; therefore the roughness of the coating applied to the pipelines will depend on the conclusions of this report, namely whether a rough or smooth interface induces greater movement and stresses within the soil. If a greater movement is induced in the soil, this shows that the soil is providing a greater resistance to the motion of the interface, which is desirable.

Andy Hill of BP exploration says that “It is of fundamental importance to understand the influence of roughness”.[3]

1.2 Previous research

Photoelastic effects have been used by Behringer and other researchers at Duke University, North Carolina to investigate the stress paths in granular material under the effect of gravity and in response to point perturbations.[4] This project uses photoelastic effects to investigate how the roughness of a surface affects the movement of particles around the soil-structure interface as well as the stresses induced by the soil shearing against that surface.

In recent work, researchers at Duke University have shown that, when shear is applied to systems of frictional particles, they exhibit entirely unanticipated states.[4] A granular system exhibits both solid and fluid characteristics, depending on the amount of energy provided to it. This project is concerned with the behaviour of grains around the soil-structure interface, as this is the area which has remained relatively unexplored as noted by Ganesan *et al.* (2013).[1]

1.2.2 Movement of grains

In the absence of continued energy input, granular materials rapidly condense into a dense state. The key stages of the "condensing" include inelastic collisions, friction, and the presence of gravity. If grains are shaken strongly enough that gravity is overcome, the shaking leads to a large number of interesting flow states. For example, when granular materials are shaken up and down with large enough accelerations, they begin to convect, something which has been observed by Eshuis *et al.* (2010).[5] Although the experiments will not involve shaking, vertical displacement of the grains may produce a similar effect, even if only momentarily.

1.2.3 Influence of roughness element shape

Research indicates that soil does not feel roughness as humans do.[1] This hypothesis will be tested. Engineers currently use relative roughness, R, as the measure for rough interfaces which, following Oliphant and Maconochie (2007)[6], can be estimated by

$$R = \frac{R_a}{D_{50}} \tag{1}$$

where R_a is the average surface roughness and D_{50} is the median grain size. The micromechanics behind the influence of interface roughness on soil-structure interface friction values are not yet understood; this will be investigated.

1.2.4 Photoelastic grains

Dense granular systems are characterised by stress chains. Forces can be detected by means of photoelasticity: when the grains deform, they rotate the polarisation of light passing through them.

Figure 1 shows a false colour image taken from an experiment by Dr Dan Howell at Duke University using this method.[7] A circular array of discs undergoes steady shearing; the coloured bands in this image give the information on the rotation of the polarisation of transmitted light. The red regions show large local force and the blue regions show weak local force. Howell uses a calibration of the photoelastic effect that takes advantage of the fact that the polarisation vector of light can actually rotate through multiple factors of pi. A similar scenario is investigated in this project in which the discs are in a rectangular array.

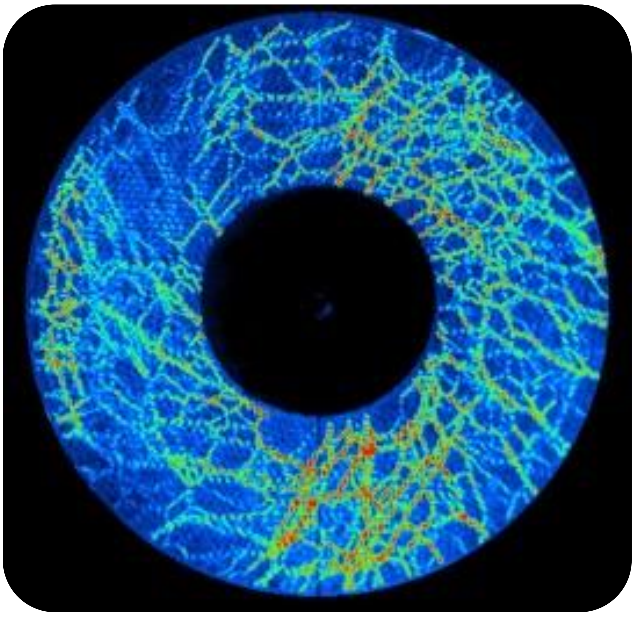

Figure 1: Stress paths in a circular array[7]

1.2.5 Jamming

Jamming is the resistance of an array of grains to applied stresses. This is the process when collections of classical particles, such as sand grains, are in a state that is mechanically rigid and stable. Many natural systems that can jam occur in nature, including granular materials, foams, colloids, and glasses. The majority of work on jamming has concentrated on particles with spherical symmetry—discs in 2D (Zhang J. *et al.* (2010)[8]), or spheres in 3D (Ovarlez *et al.* (2009)[9]). However, recent work by O'Hern *et al.* (2003)[10] and Torquato *et al.* (2001)[11] has shown the nature of jamming to be significantly altered if the shape of the particles is no longer spherical. Initial experiments carried out in this project use cylindrical discs of the same size. Some larger discs or differently-shaped discs will later be inserted into the array to avoid perfectly regular packing, eliminating jamming, therefore making the simulation more realistic.

1.3 Focus of the research and report outline

This project involves creating an assembly for shearing discs (made of acrylic or polyurethane) in order to model rough and smooth surfaces at a suitable scale for photographic imaging. How the discs displace in response to shearing by interfaces of varying roughnesses will be investigated, as well as the stresses in the discs as a result of the shearing, focusing on the soil-structure interaction with an aim to determining the amount of soil i.e. the number of discs, that interact in resisting the shearing motion. Experiments will involve several thousand discs, simulating soil particles, being sheared by a triangular interface, simulating a rough surface, which will travel across the bottom of the array. The interfaces will be interchangeable and will vary in size and shape, simulating different roughnesses. Particle Image Velocimetry (PIV) will be used to analyse the movement of acrylic discs and photoelasticity will be used to analyse the stresses induced in the array of polyurethane discs as a result of the shearing.

This report proposes to investigate the effect of surface roughness on the soil-structure interaction. The focus of this investigation is the effect that the size and shape of a shearing interface have on the movement of grains around that interface and the associated stresses in the soil matrix. Research has suggested that a higher interface friction may, counter-intuitively, be produced by a lower value of roughness.[2] This investigation sets out to test this hypothesis and to gain a deeper understanding of the behaviour of the soil at a rough boundary.

Chapter 2 explains the theory and design of the experiment, detailing its key aims as investigating the movement of grains, the effect of roughness element shape and distribution of stress. The assumptions behind the theoretical development of the project are explained as is their implementation in the experiments conducted. This chapter concludes with the hypotheses regarding the effect of roughness element size and shape on the movement of grains and the distribution of stresses within the soil.

Chapter 3 describes the apparatus and experimental techniques used in the project. The apparatus was designed and constructed specifically for this project and adaptations to the different experiments are discussed here.

In Chapter 4 the results of the experiments conducted on the acrylic and polyurethane discs are presented as vector plots for the acrylic discs and as images of the stress fields for the polyurethane discs. Graphical results are also displayed for both sets of experiments.

Chapter 5 presents a discussion of the results from the experiments conducted and discusses relationships between the behaviour of the acrylic and the polyurethane discs. This discussion goes on to test the hypotheses made in Chapter 2.

The report concludes with Chapter 6, which presents the final conclusions along with recommendations for future work, based on the advances in knowledge that have emerged from this report.

Chapter 2: Theory and design of experiment

2.1 Aims of the investigation

The project has four distinct aims.

2.1.1 To design and construct the apparatus

An apparatus is to be designed and constructed which permits the research to be undertaken. It must be able to hold a large number of discs on which PIV and photoelastic analysis can be implemented. The discs must be housed and sheared such that the shearing behaviour of the discs accurately represents the real life soil case.

2.1.2 To investigate the movement of grains

This project aims to show how the soil particles displace both at the interface and further away as a result of shearing. Particle Image Velocimetry (PIV) will be used to analyse the movement of 4,000 acrylic discs when they are sheared by interfaces of different sizes and shapes. PIV is an optical method which will track the displacement of each disc as the array is sheared and will produce a two-dimensional vector field of the discs' displacements.[12]

2.1.3 To investigate the influence of roughness element size and shape

An equilateral triangular interface will be used to shear the discs. The height of this interface will be varied to simulate different values of relative roughness for each set of discs. The angle of attack of the interface will then be changed and the effect of this change on the soil-structure interaction investigated.

2.1.4 To investigate the distribution of stress

An important issue for static granular materials concerns the way in which forces are carried through the material; dense granular systems are characterised by stress chains, which can be detected using photoelasticity. For these experiments, a system of 4,000 photoelastic discs will be used in a vertical array, between a circular polarising filter and a circular polarising viewer, which allows the observation of the stress chains as the array is sheared by interfaces of different heights and angles of attack.

2.2 Particle Image Velocimetry

Particle Image Velocimetry (PIV) is an optical technique used to visualise the flow of particles. Although originally devised for the field of experimental fluid dynamics, this displacement measurement technique can be utilised in geotechnical testing.

PIV calculates the velocity field in a plane by comparing two images containing particles separated by a very short time interval.[13] This recording of the position over time of small particles is done by implementing an interrogation scheme.[14] Individual images are divided into small subareas called “interrogation areas” or patches.[15] The local displacement vector for the images is determined by statistical methods (auto- and cross-correlation).[15] For a detailed course on PIV see Raffel *et al.* (1998)[16]. *Figure 2.2.1* presents the principles of PIV analysis.[7]

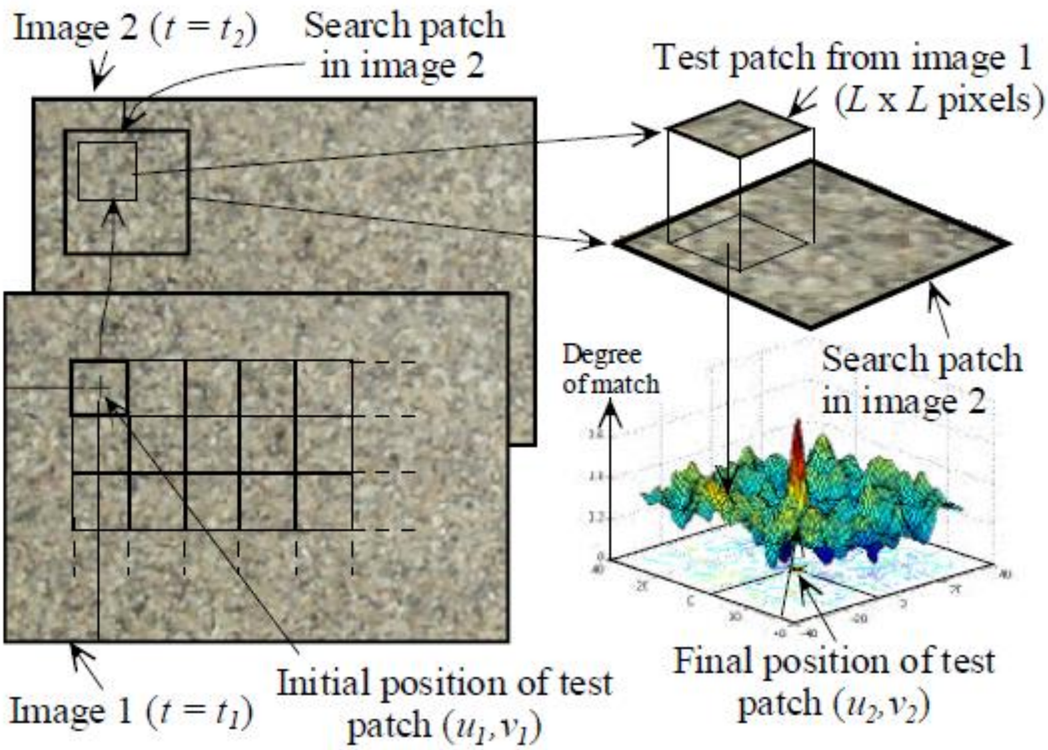

Figure 2.2.1: The principles of PIV analysis[7]

Unlike other displacement measurement techniques, such as Laser Doppler Velocimetry, PIV delivers a quantitative and instantaneous measurement of a whole plane simultaneously.

Being an optical technique, PIV is non-intrusive, with the advantage that there is no interference with the flow of particles. In intrusive techniques, the flow may be disturbed by the presence of probes.

PIV enables a large amount of information to be recorded instantaneously and simultaneously, with significantly less implementation effort than other measurement techniques.[17]

Spurious or wild vectors can occur in the vector plot if the frame rate is insufficient and if there is too much of a change between successive frames. These vectors are a result of PIV being unable to track the path of a certain particle or patch.

GeoPIV is a MatLab module, which runs at the MatLab command line. It implements PIV in a style suited to the analysis of geotechnical testing. GeoPIV takes displacement data from sequences of digital images captured during geotechnical model tests. A detailed description of the development and performance of the software is given by White (2002)[18] and Take (2002)[19].

The three inputs for GeoPIV are a launcher file, an initial mesh file and the series of images to be tested. The launcher file lists the images to be analysed and the display parameters to be used. The mesh file contains the sizes and coordinates of the initial grid of PIV patches. The output files are in the same form as the mesh files and these can be transformed into a vector plot, using the file *animate.mat*. The implementation of GeoPIV is shown in *Figure 2.2.2*.[20]

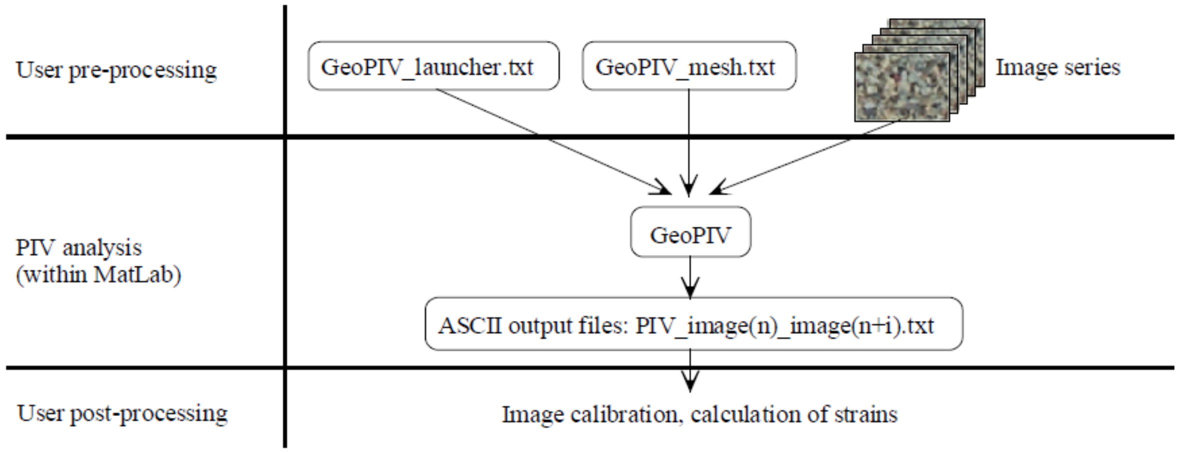

Figure 2.2.2: The implementation of GeoPIV[7]

First of all, a mesh is created from the first image using the file *geoMESHuv9.m*, as shown in *Figure 2.2.3*, where the axes are horizontal and vertical pixels.

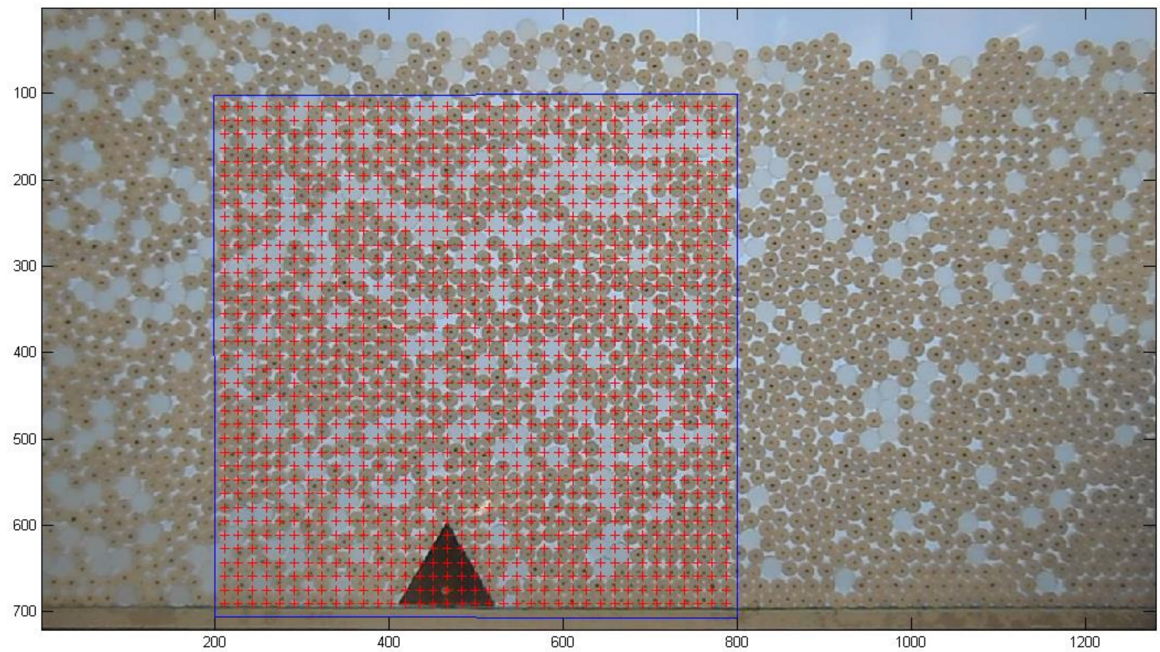

Figure 2.2.3: Mesh for PIV implementation

The launcher file is then created with suitable parameters using *launcher9.m*. *geoPIV9.m* creates files with UV positions of each point for each image and then *consolidtae9.m* is implemented, which consolidates the output and creates the output files, *PIV_image(n)_image(n+i).txt*. *animate.m* is then implemented which pieces the output files together and creates the vector plot for the sequence of images. The vector plot of the system in *Figure 2.2.3* is shown in *Figure 2.2.4* with axes of horizontal and vertical pixels.

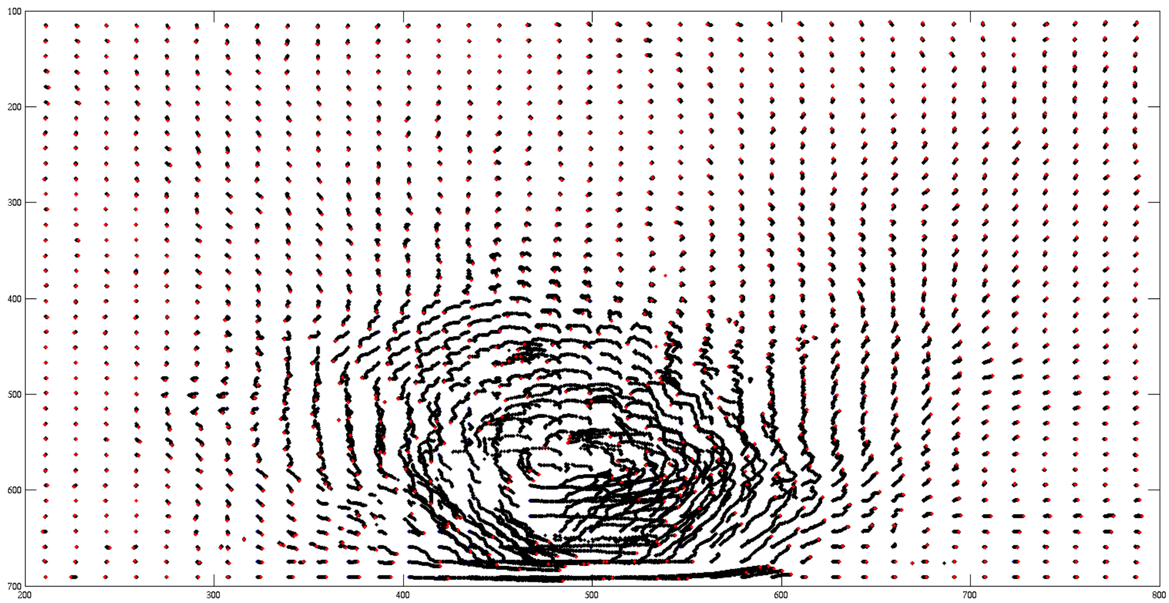

Figure 2.2.4: Vector plot output from PIV analysis

The addition of a second camera, with a viewing axis different to that of the initial camera, makes it possible to investigate the third component of the velocity vector and therefore conduct PIV in three dimensions.[17] This technique is known as stereoscopic PIV and, although not used in this project, may well be used in an extension of this project in investigating the particle movement within a three dimensional array.

2.3 Photoelasticity

Photoelasticity is a change of refractive index caused by stress. This is used as an experimental technique, which is particularly useful for members having a complicated geometry. *Photo* implies the use of light rays and *elasticity* pertains to the study of stresses and deformations in elastic bodies. Photoelasticity provides quantitative evidence of highly stressed areas and also highlights areas of low stress where the structural material is utilised inefficiently.[20] However, for quantitative analysis, calculations to separate the values of principal stresses must be carried out.[21] These calculations are tedious and deemed unnecessary for this project. Therefore qualitative analysis will be used in the place of quantitative.

Certain transparent and translucent solids exhibit birefringence when subjected to stress. Under birefringence, polarised light passing through a stressed material causes the light to separate into two waveforms, which travel at different velocities and are parallel to the directions of principal stress in the material, but perpendicular to each other. This results in the stressed material having two indices of refraction; these index values vary as a function of the stress applied. Therefore, the induced birefringence under a given stress state allows the stress distribution within the model to be examined.[22]

Photoelasticity is adaptable to both static and dynamic investigations, making it ideal for a series of experiments involving a large number of particles, some of which are moving and some of which are not.

A polariscope is required to observe the fringes induced by the stresses. If a loading frame is necessary to load a specimen, as is the case in this project, the loading frame must be placed between the first and last elements of the polariscope.

Circularly polarised light is created by combining orthogonal plane-polarised waves of equal amplitude, which are out of phase by exactly one quarter of a wavelength, as shown in *Figure 2.3.1*.[21]

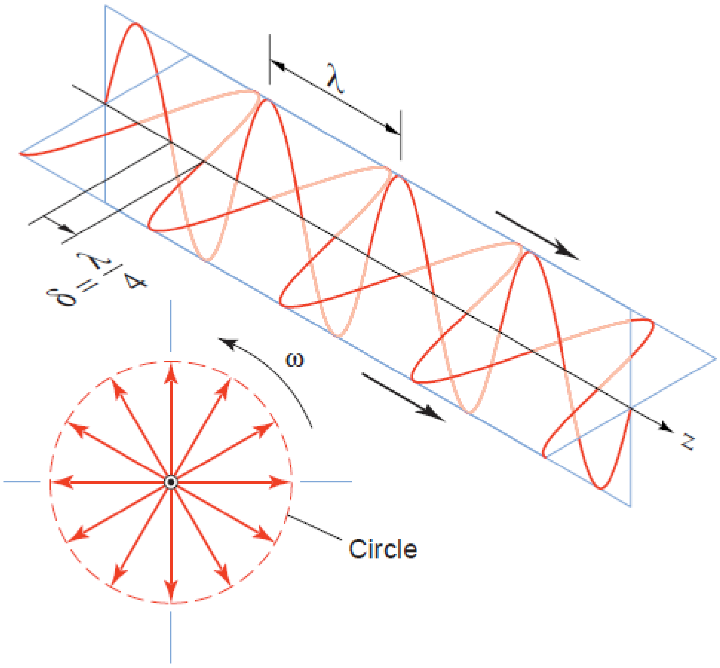

Figure 2.3.1: Circularly polarised light[21]

There are two types of fringes: isoclinics and isochromatics. Use of a circular polarising filter removes isoclinic fringes, which eliminates the problem of having to differentiate between the isoclinics and isochromatics, making analysis of the stress field significantly clearer. A circular polariscope consists of a light source, a polariser, a quarter-wave plate orientated at 45° with respect to the polariser, and an analyser, as shown in *Figure 2.3.2*.[21]

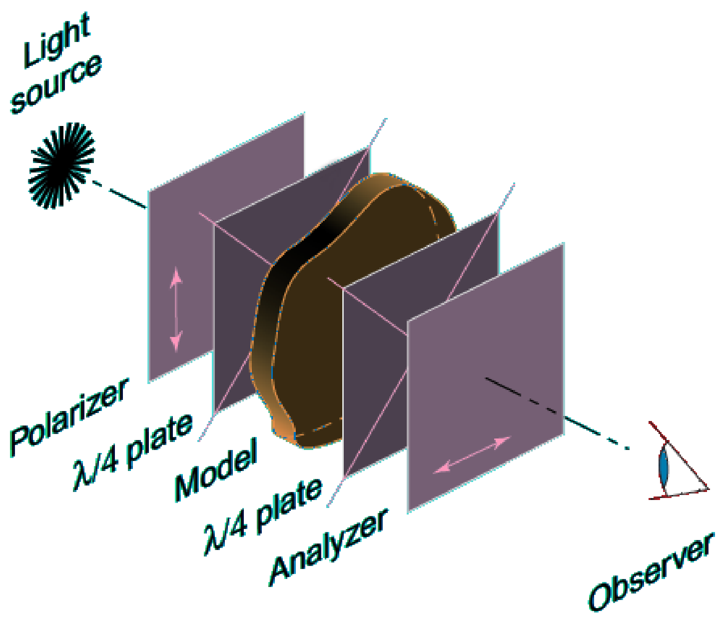

Figure 2.3.2: Circular polariscope[21]

Many polymers exhibit sufficient birefringence to be used as photoelastic specimens. Polyurethane is a photoelastic material with negligible residual stress, that is the intrinsic tension or compression which exists in the material without an external load being applied; this makes it an ideal material for the photoelastic discs.[22] This means that any observed stress (seen through diffraction patterns) is a result of experimental shearing alone.

Figure 2.3.4 shows stress paths in a polyurethane array generated from this project when loaded in the vertical plane. The more white exhibited in the stress paths, the more stress being transferred along them because they show a higher concentration of fringes.

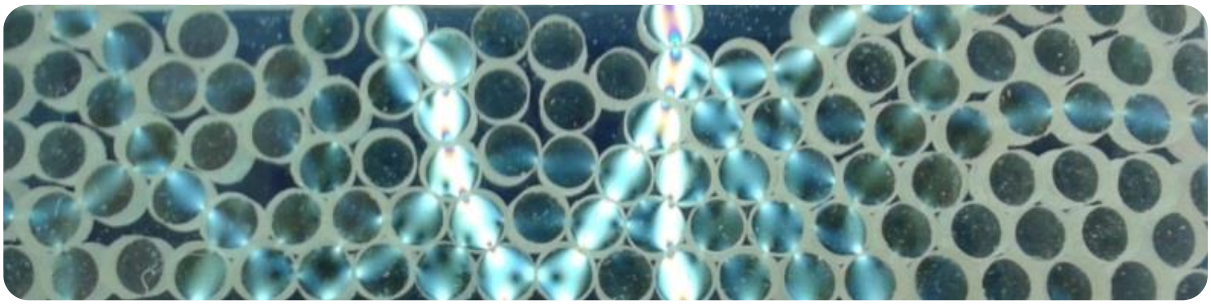

Figure 2.3.4: Stress paths in polyurethane array

2.4 Design of the experiment

The project involves two main types of experiment: shearing of photoelastic discs to investigate the stresses in the array and shearing of acrylic discs, using PIV, to track and map the displacements of the discs. The apparatus, apart from the discs, is identical for both experiments.

For both of these experiments, the effect of the size and shape of the shearing interface will be investigated. The interfaces used to investigate the effect of the height are equilateral triangles with different heights, corresponding to different values of relative roughness (see section 1.2.3 for an explanation of relative roughness). These values of relative roughness are 3.5, 5 and 6.5; dimensions of the interfaces are given in Chapter 3.

The effect of the angle of attack of the interfaces is also investigated. This is done by using interfaces of the same height, corresponding to a relative roughness of 3.5, and varying the angle of attack from 60° to 20°, as shown in *Figure 2.4.1*.

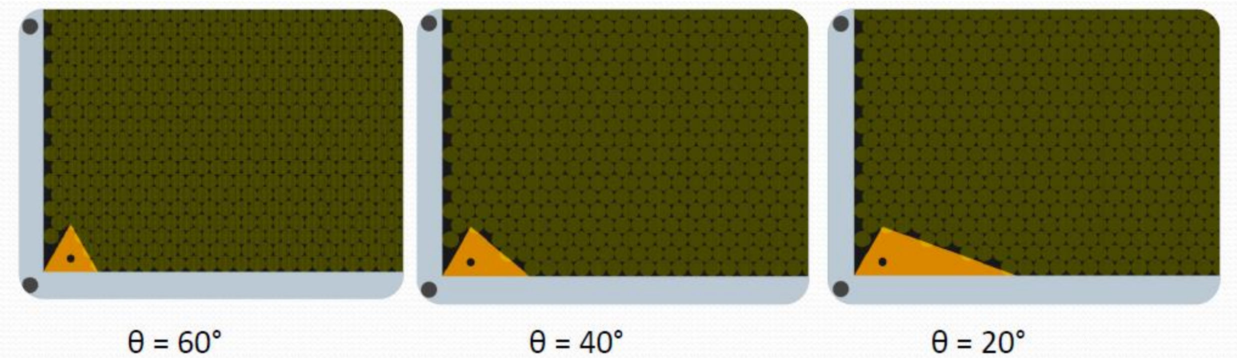

Figure 2.4.1: Interfaces with varying angle of attack

For the polyurethane discs, the changing stress paths will be observed and captured and for the acrylic discs, PIV will produce a two-dimensional vector field for shearing by each interface.

2.4.1 Adaptions to the experimental setup

The regular packing of the discs for both experiments will not perfectly simulate an array of real soil particles, which do not pack regularly. Particles of the same size will exhibit jamming (see section 1.2.5). This makes the stress field extend all of the way through the array of discs, which does not accurately simulate the behaviour of the soil under shearing. To prevent this jamming, adding a number of different shaped or sized discs to the array makes the movement of grains more realistic.

2.5 Hypotheses

The following hypotheses relate to the height of the zone of influence for a given interface. The zone of influence is taken as the area of particles where displacement or stresses are significantly affected by the movement of the interface. The height of this zone of influence is taken from the base of the interface. For the array of acrylic discs, the height of the zone of influence is taken as the height below which there is significant movement, which can be deduced form the vector plot, produced by PIV. For the polyurethane discs, the height of the zone of influence is taken as the height below which there is significant stress in the particles, which can clearly be deduced from the images of the array under shearing.

There are three hypotheses:

Hypothesis A: The height of the zone of influence is the same for the acrylic and polyurethane arrays

The height below which there if significant movement within the acrylic array is equal to the height below which there is significant stress in the polyurethane array.

Hypothesis B: The height of the zone of influence increases with the relative roughness

Relative roughness is directly proportional to the height of the interface. This hypothesis therefore states that the height of the zone of influence is proportional to the height of the interface.

Hypothesis C: The interface’s angle of attack has a negligible effect on the height of the zone of influence

Experiments conducted to test the effect of the angle of attack of the interface are conducted with interfaces of the same height and therefore the same relative roughness. It is hypothesised that the effect of the interface height is significantly more influential than its angle of attack on the behaviour of the soil particles.

Chapter 3: Apparatus and method

3.1 Apparatus components

3.1.1 Overall setup

Figure 3.1 shows the apparatus which was designed and created for the experiments in this project.

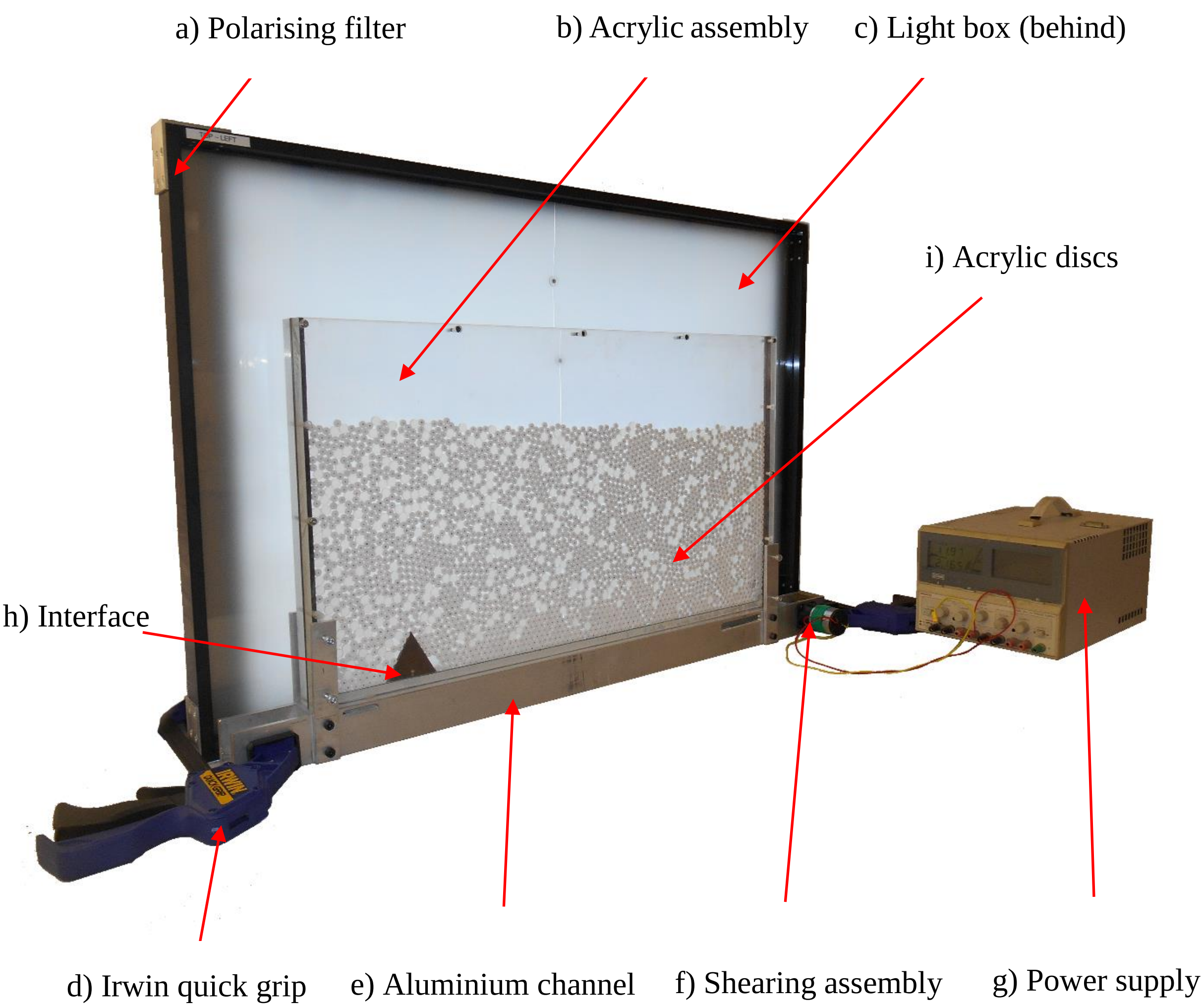

Figure 3.1: Overall setup

a: Polarising filter: 900 x 600 mm, circularly polarising, purchased

b: Acrylic assembly: two 700 mm x 400 mm x 20 mm sheets of clear acrylic, purchased

c: Light box: 820 x 570 mm, 12V, 60W, purchased

d: Irwin Quick Grip: two grips with maximum length 155 mm, purchased

e: Aluminium channel: 50.8 mm x 50.8 mm x 6.35 mm x 6.35 mm channel, purchased

f: Shearing assembly: aluminium block, motor, designed and machined for this project

g: Power supply

h: White acrylic discs: 4,000, 8 mm diameter, 3 mm thick

i: Polyurethane discs: 6,000, 6 mm diameter, 6 mm thick

j: Polarising viewer: 130 x 130mm window, circularly polarising, purchased

Figure 3.2 shows other parts of the apparatus not shown in *Figure 3.1*.

h)

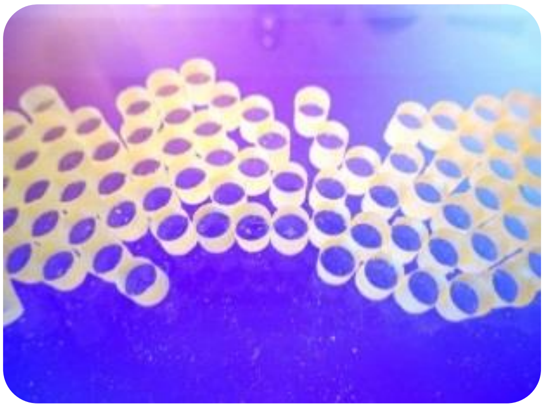

j)

Figure 3.2: Additional components

3.1.2 Acrylic discs

4,000 white acrylic discs 3 mm thick of diameter 8 mm were purchased for use in experiments to investigate the movement of particles. A dot was drawn on each disc, using a permanent marker, to make it easier for PIV to track the motion of the particles.

3.1.3 Polyurethane discs

The polyurethane discs are photoelastic which allows their stresses when sheared to be investigated, however they are less effective when used with PIV. As mentioned in the previous chapter, polyurethane is an ideal material for these discs because of the lack of inherent stresses.

3.1.3.1 Cutting out of polyurethane discs

Initially, an autonomous cutting set-up was used to cut out the 4,000 polyurethane discs, however the cutter marked the surface of the discs, rendering them useless for photoelastic imaging. Therefore, a new cutter had to be designed, which consisted of a 6 mm diameter tube containing a flat plunger with a spring behind it, which would be used in a pillar drill. It was not possible to use this equipment autonomously and so each disc had to be cut out by hand. It was important when cutting out the discs to bring the cutter into the polyurethane sheet slowly and evenly to prevent the discs being conical. The freshly cut discs had attracted dust from the cutting, which was difficult to remove, so the discs were washed in water and domestic detergent. This removed the dust and made them ready for use in the assembly. Once all of the discs were cut, it was necessary to remove any which were slightly conical in shape or any which were not perfectly circular in cross-section as these discs would either contain inherent stresses or would not sit well in the apparatus, corrupting the results in each case.

3.1.4 Larger sized discs

To prevent jamming (see section 1.2.5), different sized discs were added to both the polyurethane and acrylic discs. For the polyurethane array of discs, white acrylic discs of diameter 8 mm and thickness 6 mm were added and for the acrylic array, silicone discs of diameter 10 mm and thickness 3 mm were added.

3.1.5 Interfaces

Interfaces are all made of Tufnol, which is woven cotton fibre and epoxy resin. They are 4 mm thick with 2 mm diameter holes drilled for attachment to the traversing mechanism. Recall the definition of relative roughness from section 1.2.3:

$$R = \frac{R_a}{D_{50}} \tag{1}$$

where R_a is the average surface roughness and D_{50} is the median grain size.[6] Based on this equation, and taking D_{50} = 6 mm for the polyurethane discs and D_{50} = 8 mm for the acrylic discs, the height of the interfaces to be used can be calculated. *Figure 3.3* shows the dimensions of a standard interface and *Table 3.2* gives the dimensions of all of the interfaces used in the project. *Figure 3.4* shows the interfaces used for the polyurethane array.

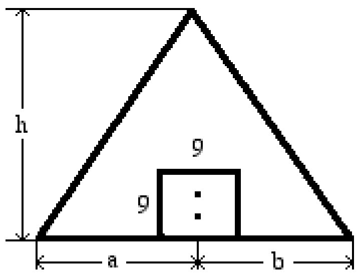

Figure 3.3: Dimensions

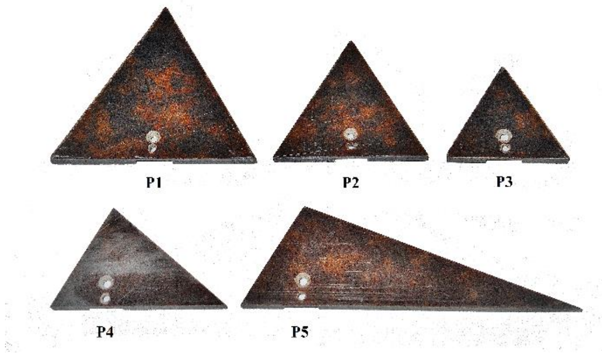

Figure 3.4: Interfaces for polyurethane

Interface	a /mm	b /mm	Interface height, h/mm	Relative roughness	Angle of attack
A1	30	30	52	6.5	60°
A2	23	23	40	5.0	60°
A3	16	16	28	3.5	60°
A4	16	33	28	3.5	40°
A5	16	77	28	3.5	20°
P1	22.5	22.5	39	6.5	60°
P2	17.5	17.5	30	5.0	60°
P3	12	12	21	3.5	60°
P4	12	25	21	3.5	40°
P5	12	58	21	3.5	20°

3.1.5 Shearing assembly

Ensuring that the discs could be sheared in a uniform and precise manner was a concern. A number of mechanisms were considered but a worm screw was deemed the best option. A length of studding along the bottom of the acrylic assembly is constrained in the longitudinal direction but is able to rotate. A motor attached to a variable voltage power supply rotates this length of studding along which an aluminium block moves, however the block is constrained against rotation by the sides of the channel in which it sits. It has a vertical protrusion to which a number of different interfaces can be attached.

3.1.7 3D CAD model using ProEngineer

The 3D CAD model (*Figure 3.5*) facilitated the designing of new components and the dimensions were transferred directly which enabled the interaction between components to be investigated without unnecessary manufacture. The majority of components were modelled in CAD before being constructed. The 3D model was created by the author and every component was produced from scratch.

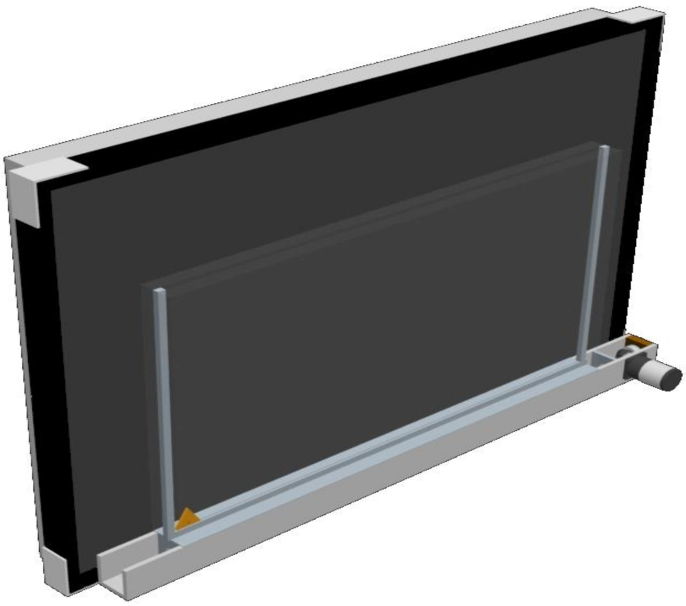

Figure 3.5: 3D CAD model

3.2 Issues overcome

Before any results could be obtained, the bespoke apparatus had to be designed and constructed. It was essential that the discs would be held securely whilst allowing change between the two sets of discs, which are of different thicknesses. The set-up also had to facilitate changing between different interfaces with minimal disruption. Where possible, materials were sourced from existing stock however, given the unique nature of the apparatus and its considerable size, most of the material had to be ordered in and cut to size. Apart from the filing down of components and similar adjustments which are natural for a bespoke apparatus, the following issues were encountered.

3.2.1 Assembling the apparatus

When designing each component, it was important to consider how the entire apparatus would fit together. This included counter-boring any holes drilled in the acrylic sheets to ensure the surface was flush. Although drawings were produced of the apparatus, much of the construction came down to measuring dimensions off the existing apparatus.

3.2.2 Restraining the apparatus

The apparatus can be unstable and therefore it is essential to restrain the apparatus from tipping, especially since the acrylic assembly is so heavy. The apparatus is held together with Irwin Quick Grips at the base, which prevents any single component from tipping independently. The light box, which sits at the back of the apparatus, is attached to the wall, preventing everything from tipping towards the observer.

3.2.3 Housing the discs

Given that the two sets of discs used in the project were different thicknesses, different thicknesses of separators for the acrylic sheets were manufactured. These separators were 10 mm wide and 7 mm thick for the polyurethane discs and 4 mm thick for the acrylic discs.

A difficulty encountered was preventing the discs from dropping out of the bottom of the acrylic housing whilst be able to shear them. This was overcome by sticking a thin strip of polymer resin to the inside face of the two acrylic sheets, creating a 1 mm gap for the vertical interface bracket to pass through. This allowed the interface assembly to move along the bottom of the discs whilst preventing any discs from dropping out of the bottom.

3.3 Experimental method

3.3.1 Acrylic discs

1. Videos are taken of the discs as they are sheared using a compact digital camera.
2. A 20-second exert is extracted using the program *ffmpeg*, which snips the original video. This 20-second exert must accurately represent the behaviour of the discs to shearing by that interface.
3. This video is split into frames. In this case, one in every four frames is extracted from a video recorded at 24 frames/second.
4. These frames are placed on the MatLab path.
5. geoPIV is implemented with the following commands
    a) geoMESHuv("A1.txt",32,16)
    b) launcher9
    c) geoPIV9
    d) A1=consolidate9
    e) Animate(A1)
6. The vector field output is saved as a .tiff image.
7. This image is rescaled to have the same aspect ratio as the mesh and the background colour is removed to enable overlaying this plot with an image of the discs sheared. This is done using the program *GIMP*.
8. The first frame is cropped to be the same size as the mesh used in the PIV analysis.
9. The vector field and image of the discs are overlaid.
10. From this overlaid image, it is possible to measure the height of the zone of influence within the array of discs relative to the height of the interface.

3.3.2 Polyurethane discs

1. Videos are taken of the discs as they are sheared using a compact digital camera.
2. Frames are selected from a video for each interface which accurately represent the behaviour of the discs to shearing by that interface.
3. From these frames, it is possible to measure the height of the zone of influence within the array of discs relative to the height of the interface.

Chapter 4: Results

Results are produced using the methods described in section 3.2. All images and vector plots are to scale. The vector plots for the acrylic discs are at a scale of 2:3 and the images for the polyurethane discs are at a scale of 2:7. The height of the interface and the height of the zone of influence is marked on each vector plot and photoelastic image. All dimensions are in mm.

4.1 Acrylic discs

The zone of influence for the PIV vector plots is taken as the maximum height above the datum at which there is noticeable horizontal movement of the discs. Horizontal movement can be seen as horizontal black lines in the following figures.

Figures 4.1.1-4.1.5 present the PIV vector plots of particle movement for each interface. *Tables 4.1.1-4.1.5* summarise the results for each interface.

Table 4.1.6 presents the height of the zone of influence for each interface.

Figure 4.1.6 is a plot of the height of the zone of influence against the relative roughness for each interface from three trials.

Figure 4.1.7 is a plot of the height of the zone of influence against the angle of attack of an interface with a relative roughness of 3.5 for each interface from three trials.

For each interface, three separate test trials were undertaken to generate three separate PIV plots which were then analysed. Only one of these plots is shown for each interface but the heights of the zones of influences for all of the plots are presented in the respective tables.

Figure 4.1.1: Interface A1

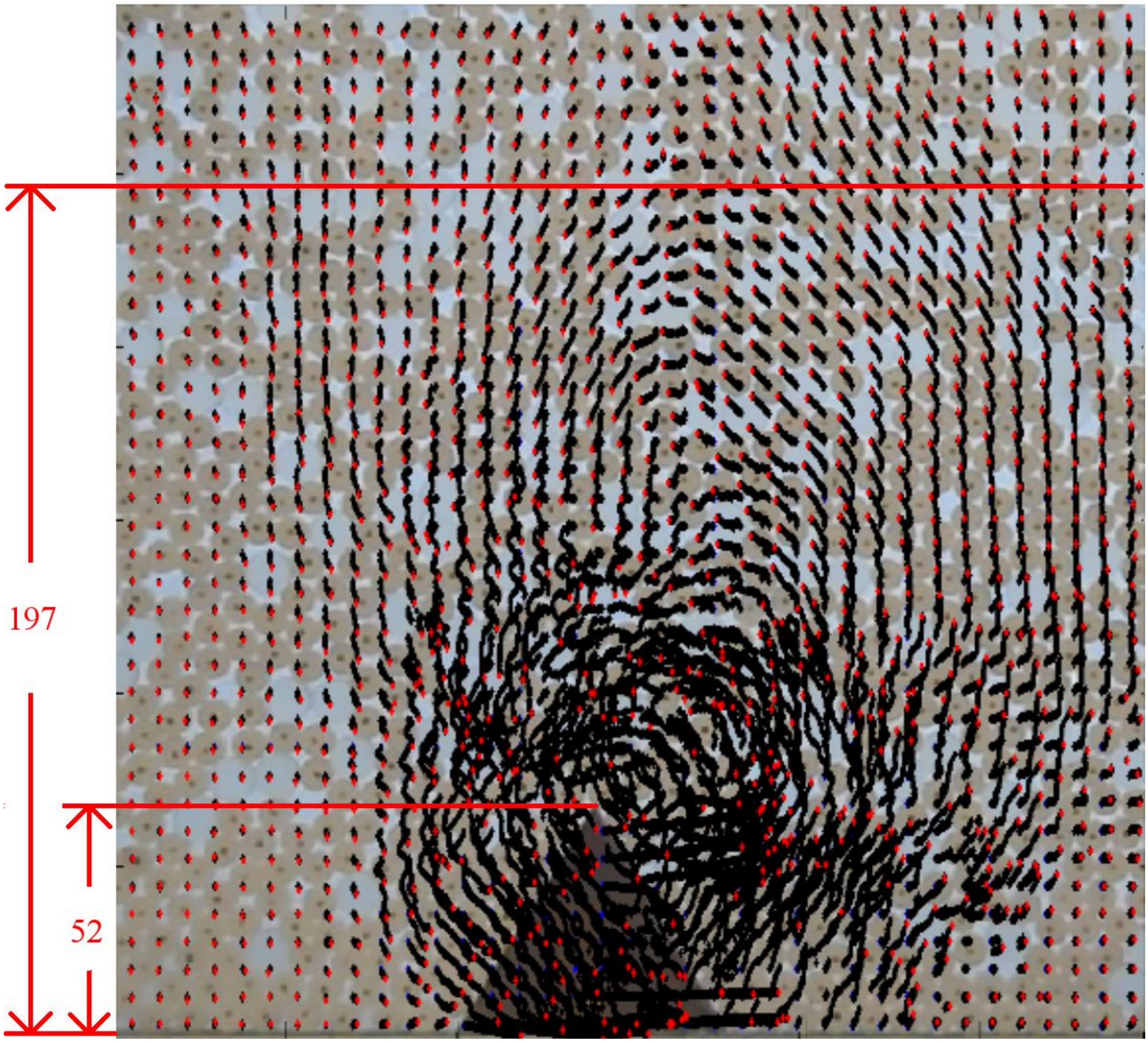

Table 4.1.1: Interface A1

Height of interface /mm	Angle of attack	Height of zone of influence /mm			
		1	2	3	Average
52	60º	197	197	191	195

Figure 4.1.2: Interface A2

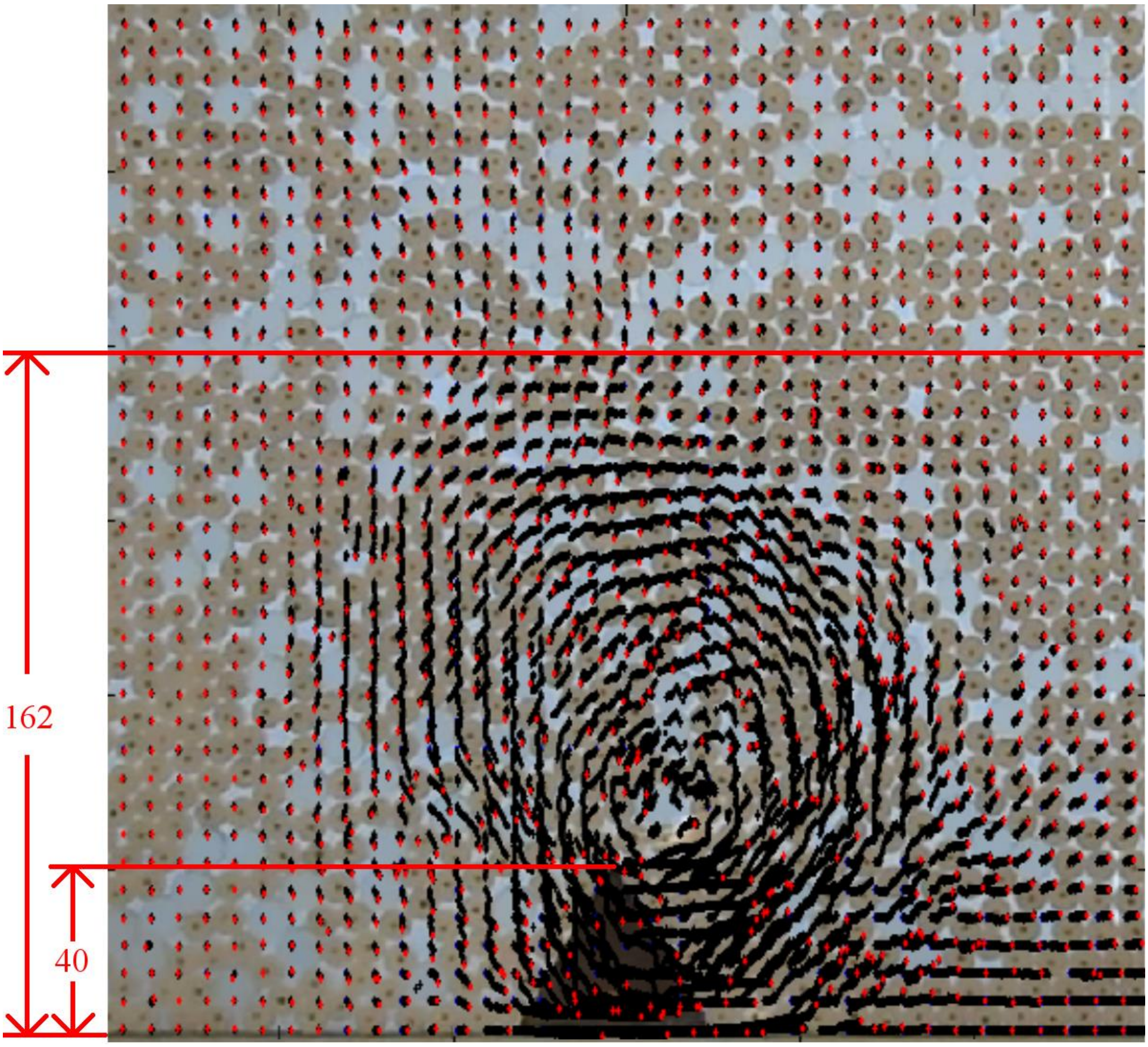

Table 4.1.2: Interface A2

Height of interface /mm	Angle of attack	Height of zone of influence /mm			
		1	2	3	Average
40	60º	162	145	147	151

Figure 4.1.3: Interface A3

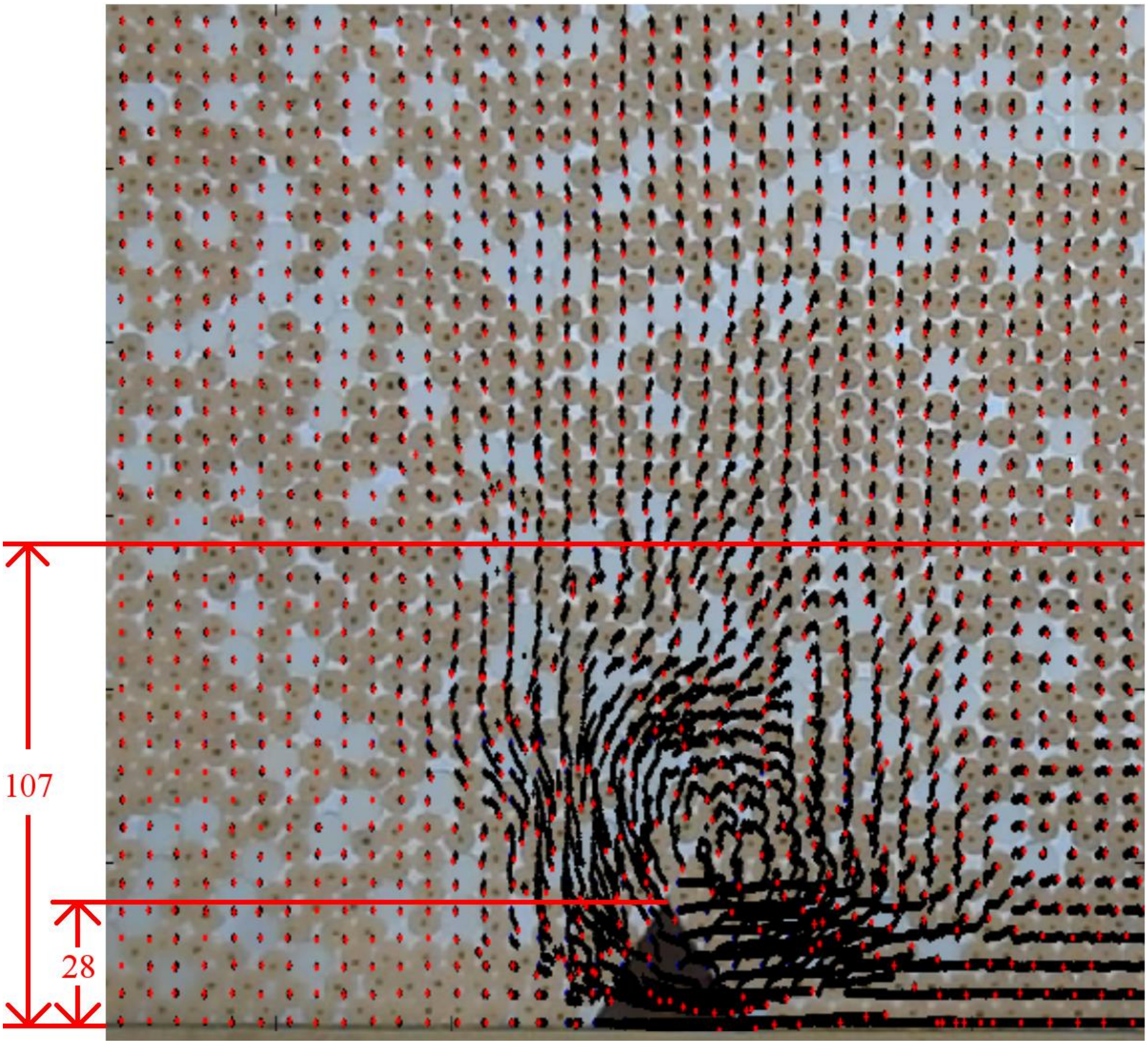

Table 4.1.3: Interface A3

Height of interface /mm	Angle of attack	Height of zone of influence /mm			
		1	2	3	Average
28	60º	107	101	100	103

Figure 4.1.4: Interface A4

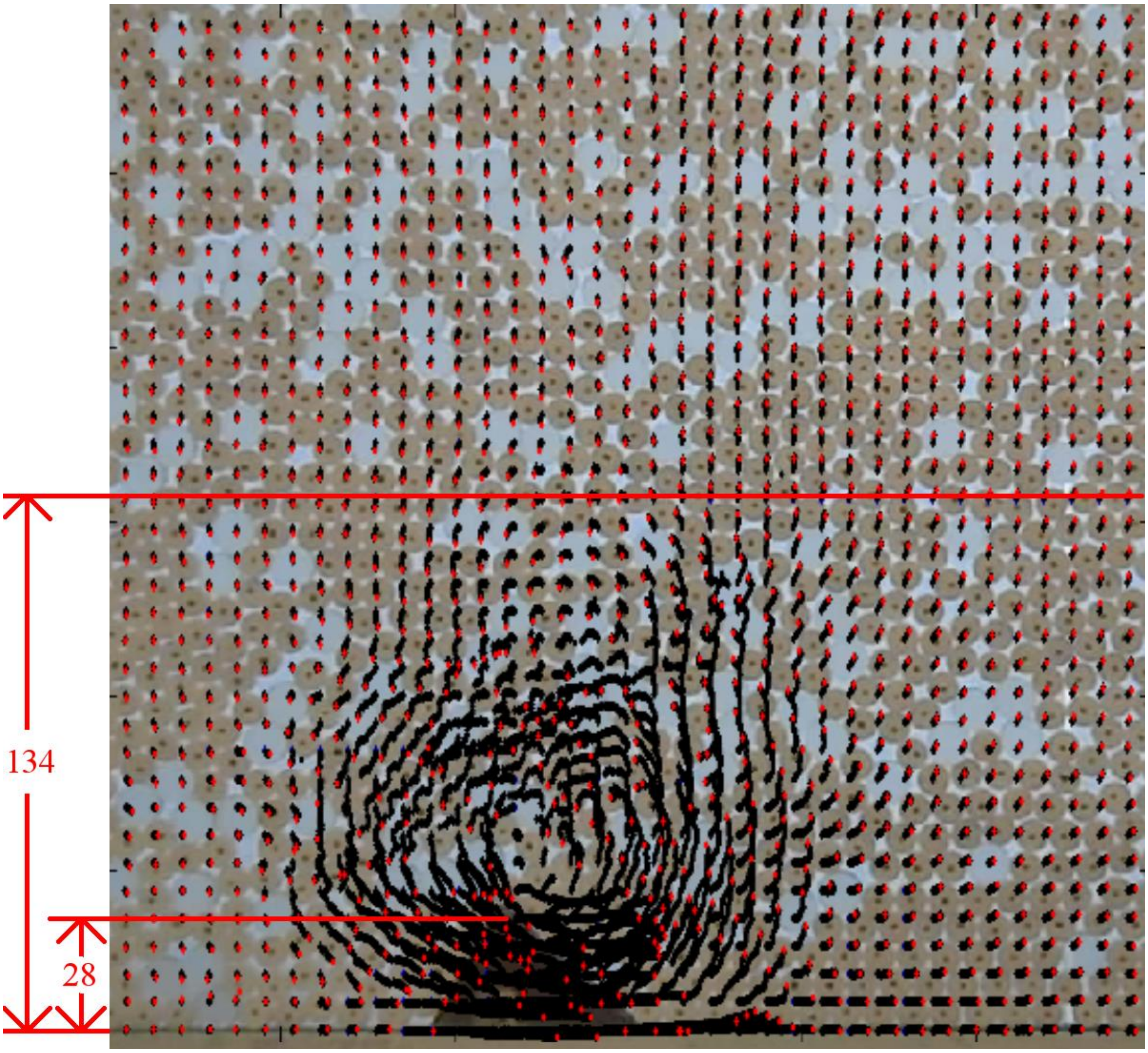

Table 4.1.4: Interface A4

Height of interface /mm	Angle of attack	Height of zone of influence /mm			
		1	2	3	Average
28	40º	134	101	104	113

Figure 4.1.5: Interface A5

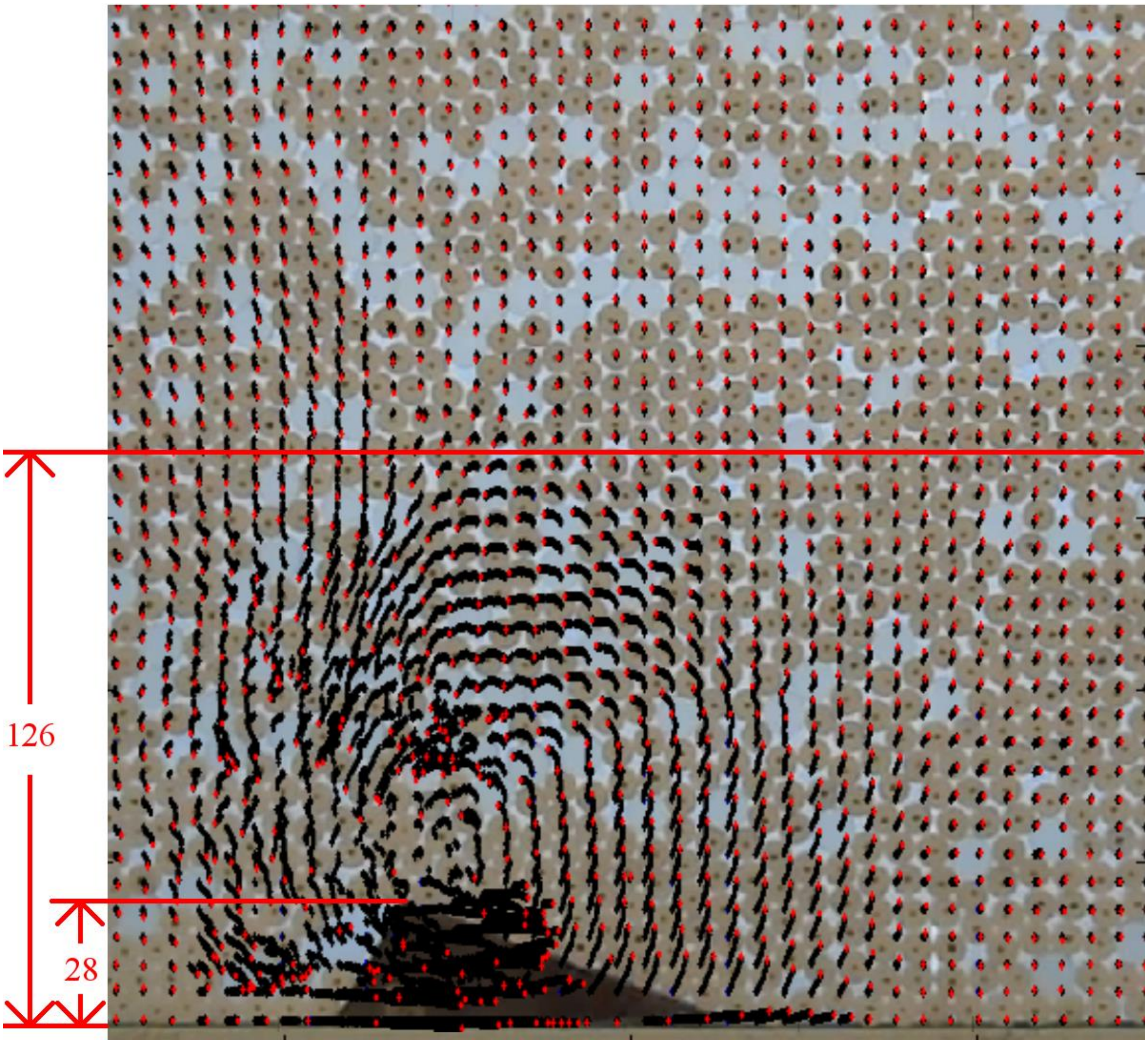

Table 4.1.5: Interface A5

Height of interface /mm	Angle of attack	Height of zone of influence /mm			
		1	2	3	Average
28	20º	126	131	123	127

Table 4.1.6: Height of the zone of influence for each interface

Interface	Interface height /mm	Relative roughness	Angle of attack	Height of zone of influence /mm			
				1	2	3	Average
A1	52	6.5	60°	197	197	191	195
A2	40	5.0	60°	162	145	147	151
A3	28	3.5	60°	107	101	100	103
A4	28	3.5	40°	134	101	104	113
A5	28	3.5	20°	126	131	123	127

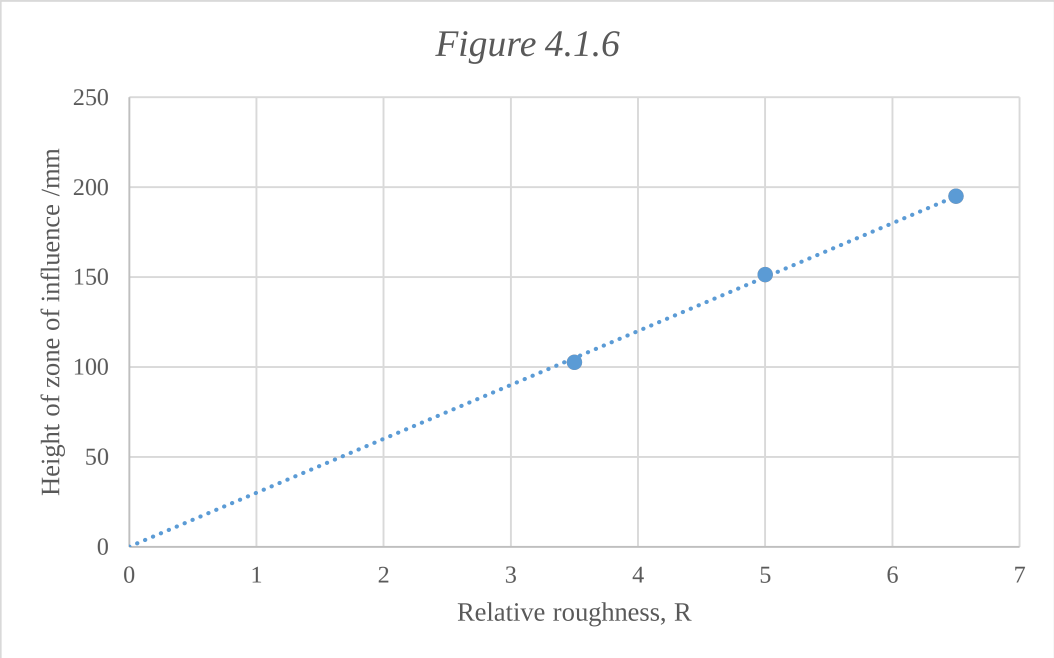

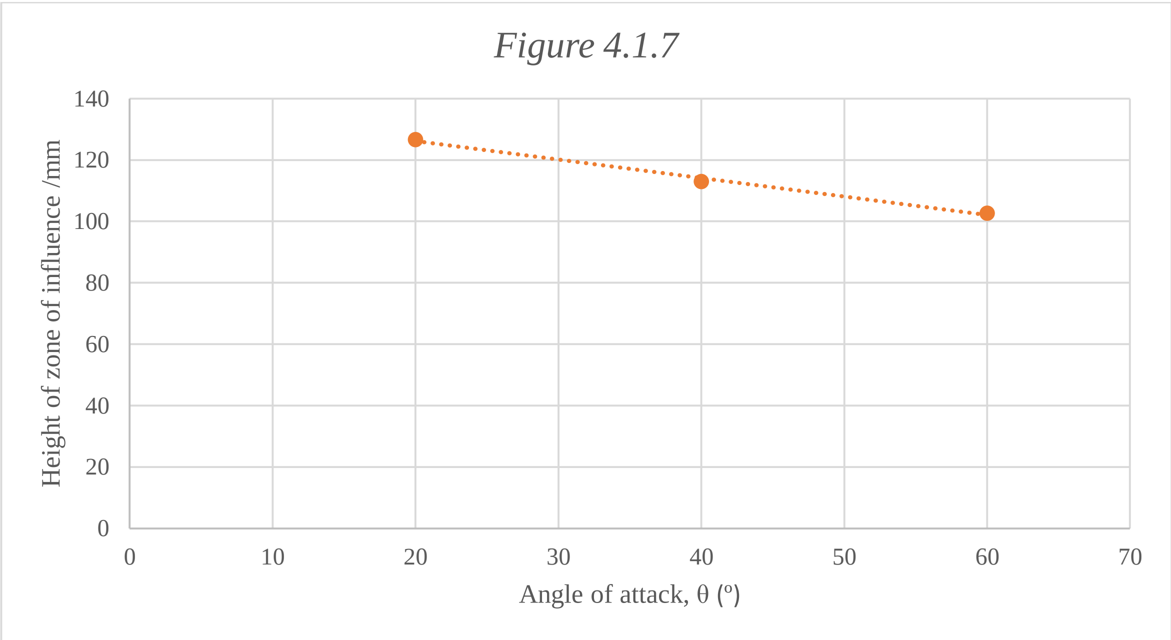

4.2 Polyurethane discs

Figures 4.2.1-4.2.5 present snapshots from videos taken of the polyurethane array being sheared by each interface. These figures show the extent of the stresses throughout the polyurethane disc matrix and the height of the zone of influence in each case is presented in *Tables 4.2.1-4.2.5*.

Figure 4.2.6 is a plot of the height of the zone of influence against the relative roughness for each interface from three trials.

Figure 4.2.7 is a plot of the height of the zone of influence against the angle of attack of an interface with a relative roughness of 3.5 for each interface from three trials.

Figure 4.2.1: Interface P1

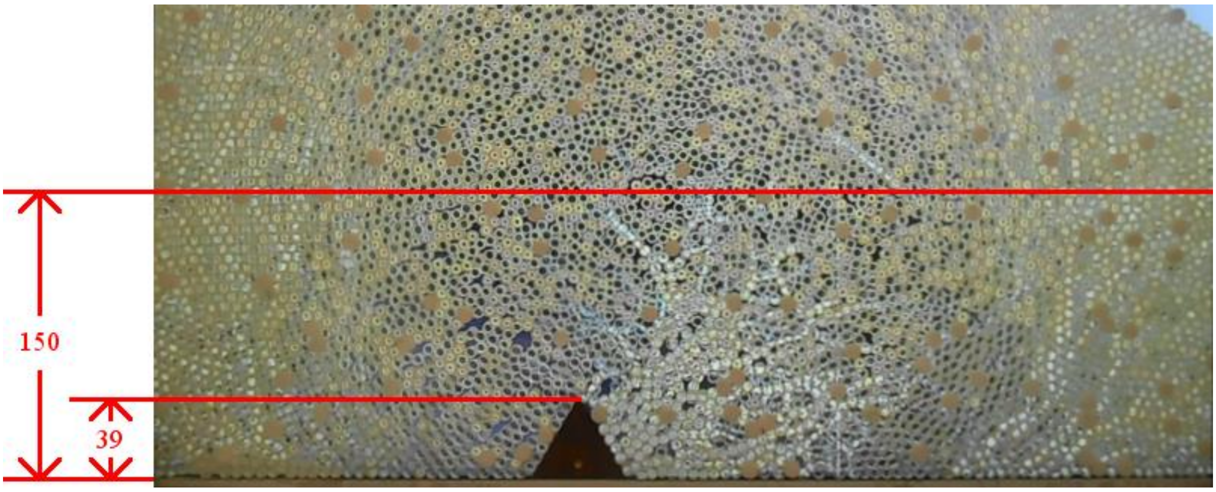

Table 4.2.1: Interface P1

Height of interface /mm	Angle of attack	Height of zone of influence /mm			
		1	2	3	Average
39	60º	150	160	150	153

Figure 4.2.2: Interface P2

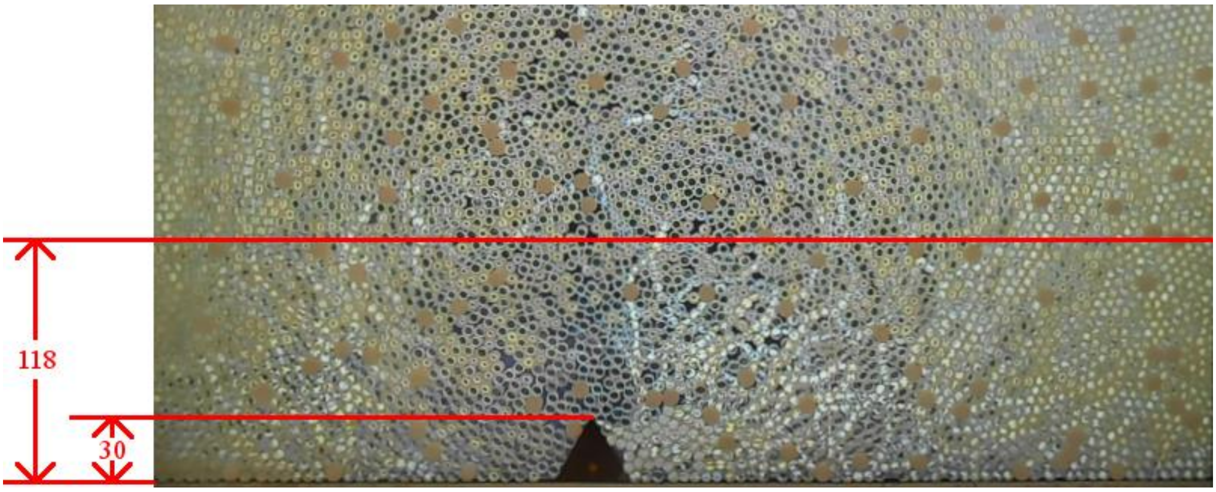

Table 4.2.2: Interface P2

Height of interface /mm	Angle of attack	Height of zone of influence /mm			
		1	2	3	Average
30	60º	118	124	109	117

Figure 4.2.3: Interface P3

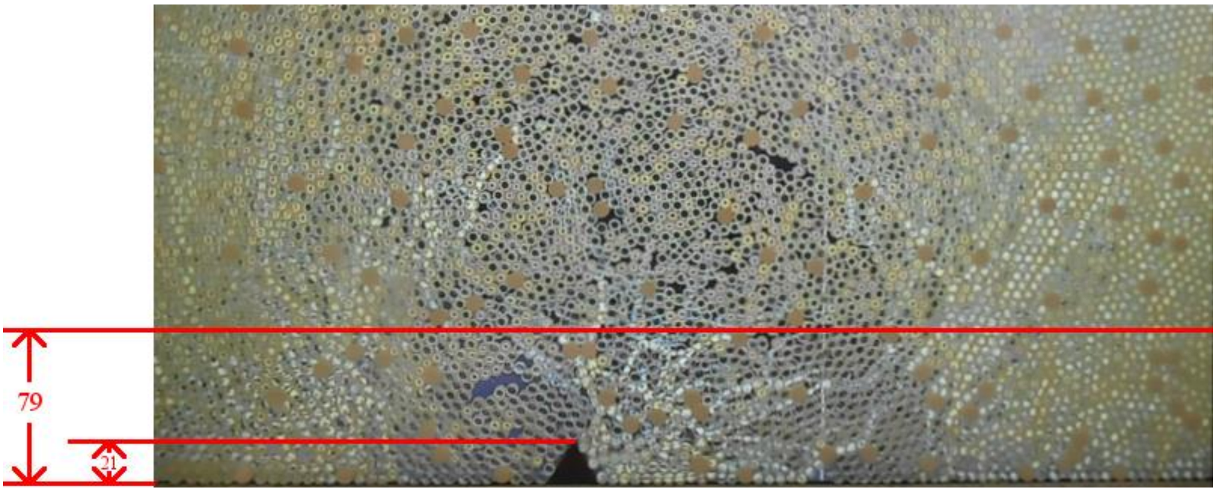

Table 4.2.3: Interface P3

Height of interface /mm	Angle of attack	Height of zone of influence /mm			
		1	2	3	Average
21	60º	79	86	82	82

Figure 4.2.4: Interface P4

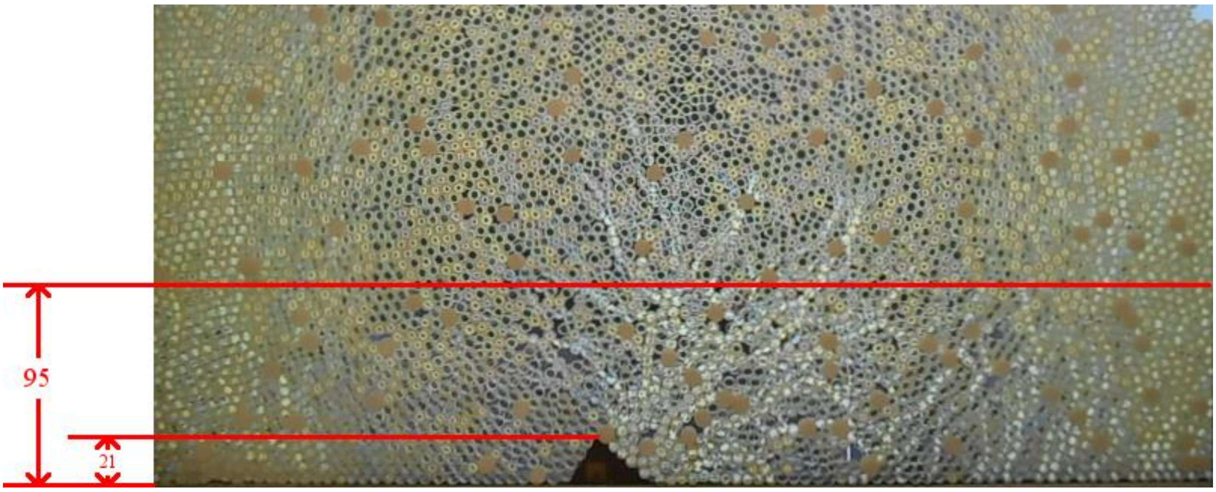

Table 4.2.4: Interface P4

Height of interface /mm	Angle of attack	Height of zone of influence /mm			
		1	2	3	Average
21	40º	95	93	96	95

Figure 4.2.5: Interface P5

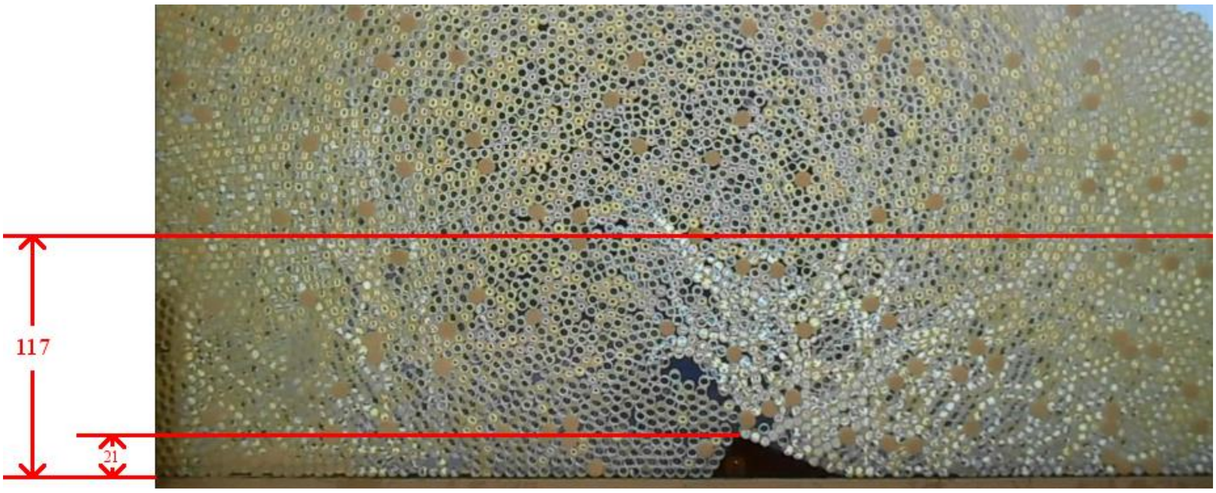

Table 4.2.5: Interface P5

Height of interface /mm	Angle of attack	Height of zone of influence /mm			
		1	2	3	Average
21	20º	117	111	99	109

Table 4.2.6: Height of the zone of influence for each interface

Interface number	Interface height /mm	Relative roughness	Angle of attack	Height of zone of influence /mm			
				1	2	3	Average
P1	39	6.5	60°	150	160	150	153
P2	30	5.0	60°	118	124	109	117
P3	21	3.5	60°	79	86	82	82
P4	21	3.5	40°	95	93	96	95
P5	21	3.5	20°	117	111	99	109

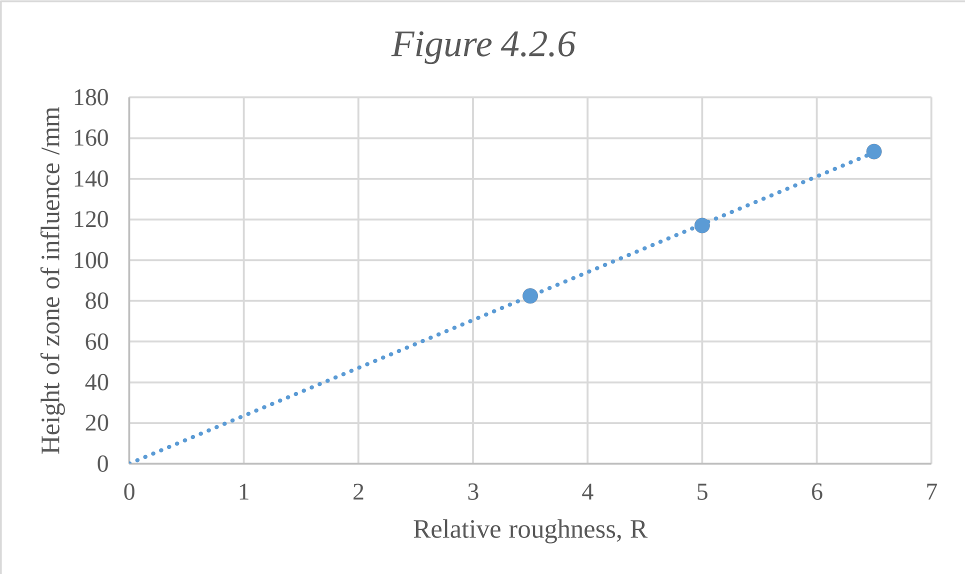

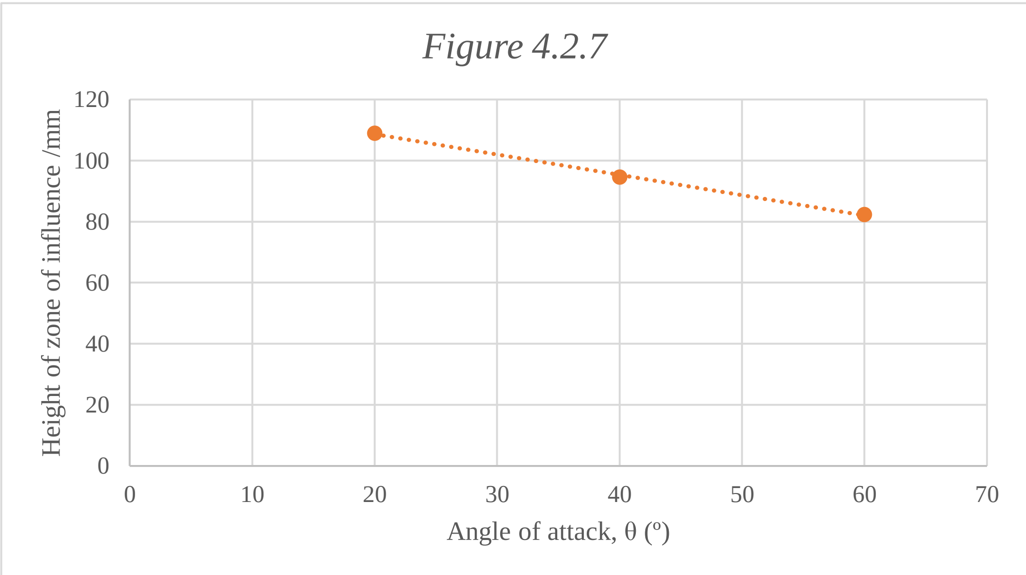

Chapter 5: Discussion

5.1 Testing the hypotheses

5.1.1 Testing Hypothesis A

> The height of the zone of influence is the same for the acrylic and polyurethane arrays

For this first hypothesis to be true, the height of the zone of influence must be the same for both tests.

Table 5.1 presents the average height of the zone of influence for the acrylic and the polyurethane discs with an angle of attack of 60º. *Figure 5.1* shows this data graphically.

Table 5.1 Comparison of average height of the zone of influence

Relative roughness	Average height of zone of influence /mm	
	Acrylic	Polyurethane
6.5	195	153
5.0	151	117
3.5	103	82

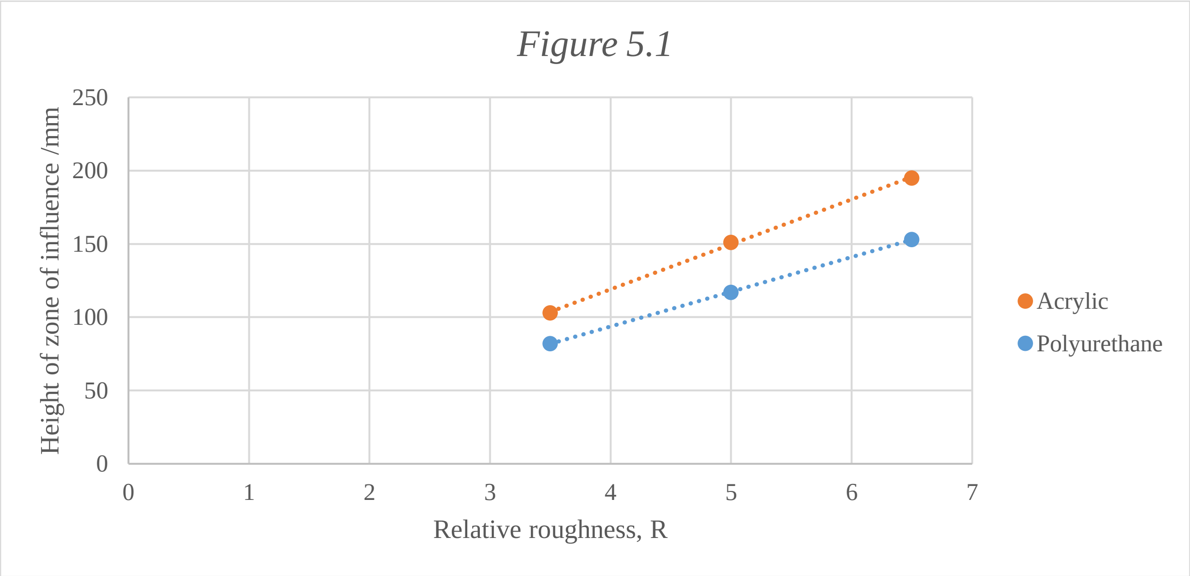

Clearly, although these two series of data show a very similar relationship, the comparison is not close enough to conclude that the heights for the two tests to be the same.

A comparison between the acrylic and polyurethane experiments should be made with normalised values of the height of the zone of influence since the height of this zone scales with the diameter of the discs and the two sets of discs have different diameters. Normalised values are computed by dividing the height of the zone of influence by the diameter of the discs used, which is 8 mm for the acrylic discs and 6 mm for the polyurethane. These values are presented in *Table 5.2*. *Figure 5.2* displays these normalised results graphically.

Table 5.2: Comparison of normalised average height of the zone of influence

Relative roughness	Average height of zone of influence /mm		Normalised average height of the zone of influence	
	Acrylic	Polyurethane	Acrylic	Polyurethane
6.5	195	153	24.4	25.5
5.0	151	117	18.9	19.5
3.5	103	82	12.9	13.7

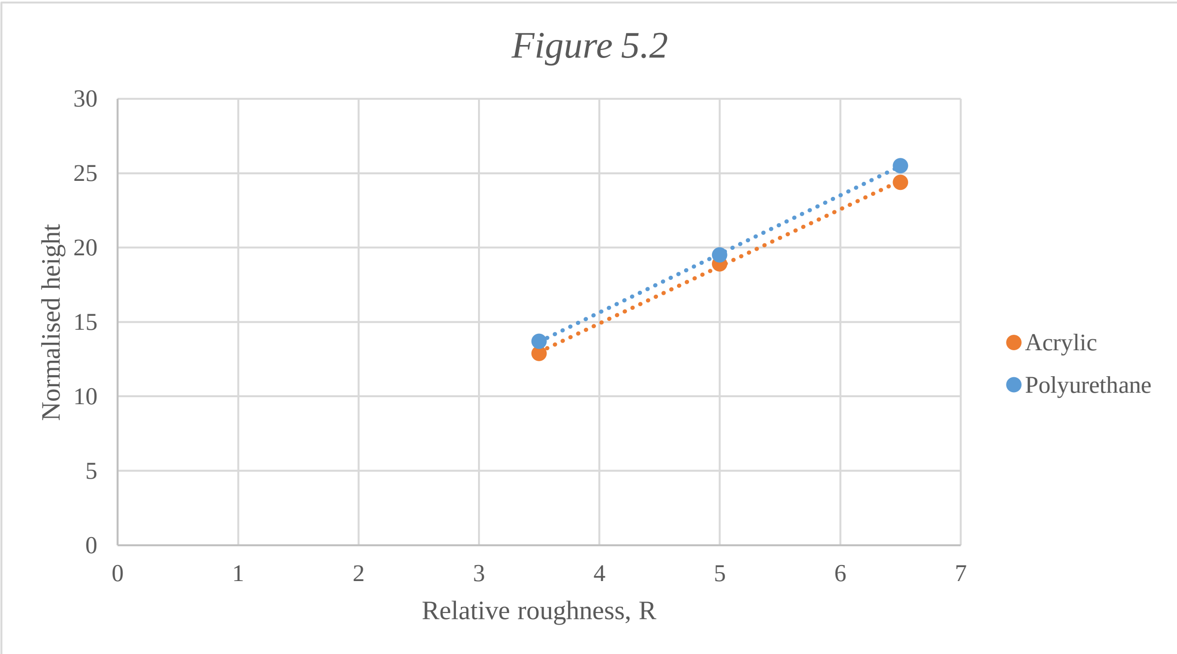

From *Figure 5.2*, the normalised heights of the zone of influence for the acrylic and polyurethane test are clearly very similar. The standard deviation between the acrylic and polyurethane results is found to be less than 10%, which is an acceptable confidence interval for this hypothesis, given the experimental nature of this test and the large scope for human errors. Therefore, it can be stated that the height below which there is significant movement within the acrylic array is equal to the height below which there is significant stress in the polyurethane array within a reasonable level of accuracy.

The reason for which there is a difference, however small, between the heights calculated for the different tests, is that, at the boundaries of the zone of influence of stress, the stresses, although noticeably present, are not high enough to cause movement of the discs, as seen in the acrylic tests.

5.1.2 Testing hypothesis B

The height of the zone of influence increases with the relative roughness

It is clear from the tests on both the acrylic and the polyurethane discs that the height of the zone of influence increases with relative roughness for interfaces with a constant angle of attack. This shows that for higher values of relative roughness, the soil resists the motion of the interface with a larger volume of soil.

To test the nature of the relationship between the height of the zone of influence and the relative roughness, it is necessary to divide the height of this zone by the relative roughness of the interface. As for the first hypothesis, normalised values are calculated and used in the comparison. *Table 5.3* and *Figure 5.3* present this information.

Table 5.3: Ratio of the height of zone of influence to relative roughness

Relative roughness	Normalised average height of zone of influence		Average height of zone of influence/relative roughness	
	Acrylic	Polyurethane	Acrylic	Polyurethane
6.5	24.4	25.5	3.75	3.92
5.0	18.9	19.5	3.78	3.90
3.5	12.9	13.7	3.68	3.90

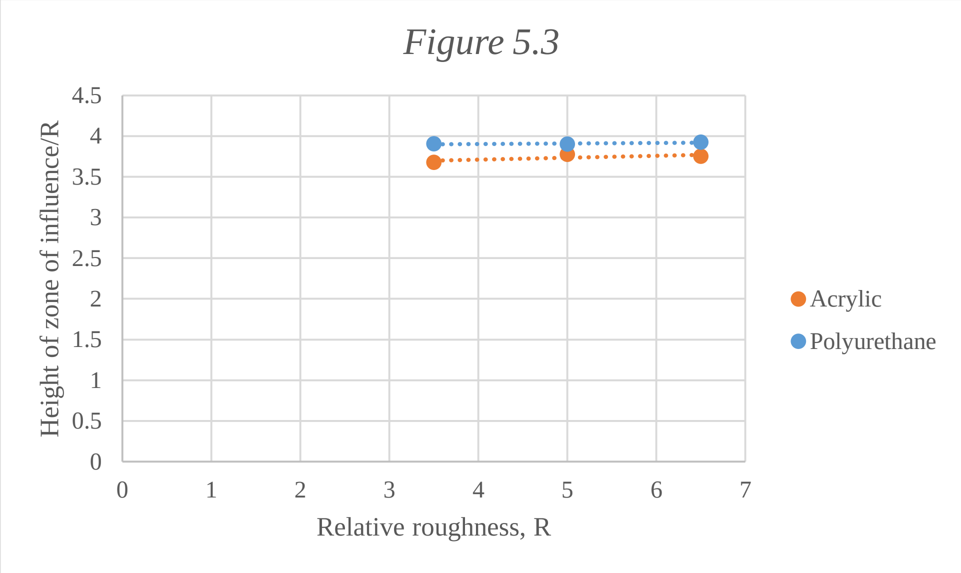

This data gives an average ratio of the normalised height of the zone of influence to the relative roughness of 3.73 for the acrylic discs and 3.91 for the polyurethane discs. These results are very close in value, showing a strong relationship between the two experiments, with a standard deviation of 0.09. The data in *Table 5.3* and *Figure 5.3* also show a high level of consistency within the results for each set of discs. The reason for which the ratio is higher for the polyurethane discs than for the acrylic discs is the same as for the first hypothesis.

This hypothesis is true because not only does the height of the zone of influence scale with the relative roughness of the interface but this ratio is the same, within a reasonable confidence interval, for both the acrylic and polyurethane discs.

5.1.3 Testing hypothesis C

> The interface's angle of attack has a negligible effect on the height of the zone of influence

There is a clear relationship between the height of the zone of influence and the angle of attack for both sets of discs, as shown in *Table 5.4* and *Figure 5.4* below. This hypothesis is therefore false. The relationship between these two variables is unexpected. What can be seen from the results for both the acrylic and polyurethane tests is that an increased angle of attack leads to a reduction in the height of the zone of influence.

Table 5.4: The effect of the angle of attack on the height of the zone of influence

Angle of attack	Average height of zone of influence /mm		Normalised average height of the zone of influence	
	Acrylic	Polyurethane	Acrylic	Polyurethane
60°	103	82	12.9	13.7
40°	113	95	14.1	15.8
20°	127	109	15.9	18.2

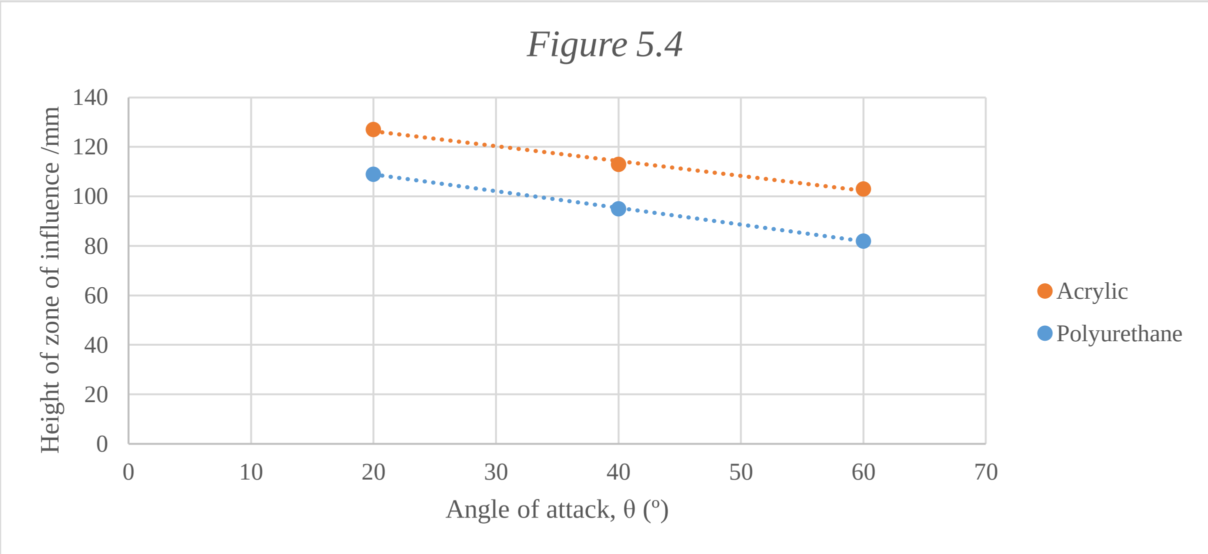

Normalising the results by dividing the average height of the zones of influence by the disc diameter does bring the two sets of data closer together but also increases the angle between the linear trend lines for the two sets of discs, as shown in *Figure 5.5*.

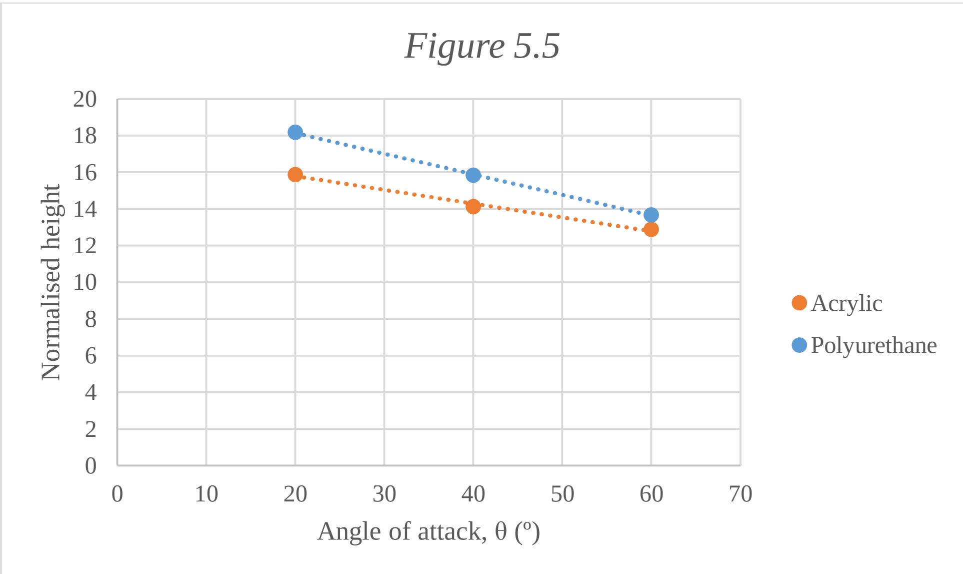

The next step beyond establishing that such a relationship exists is to deduce its significance compared to the relationship found between the height of the zone of influence and the relative roughness. It was hypothesised that the effect of the interface height was significantly more influential than its angle of attack on the behaviour of the soil particles. It will only be possible to compare the effects of these two variables from the data collected here if it is assumed that both the variation in relative roughness used for the tests and the difference in the angles of attack used for the tests are deemed to be similar. Assuming this to be the case, the difference in the height of the zone of influence between an interface with an angle of attack of 60º and 20º must be significantly less than the difference in height of the zone of influence between an interface of relative roughness 6.5 and one of relative roughness 3.5. Taking for each of these cases the average normalised difference in height of the acrylic and polyurethane results, *Table 5.5* shows the calculations.

Relative roughness	Angle of attack	Average height of the zone of influence /mm			Difference in height of the zone of influence /mm
		Acrylic	Polyurethane	Average	
6.5	60°	195	204	200	94
3.5	60°	103	109	106	
3.5	20°	127	145	136	30

Table 5.5: A comparison of the effect of relative roughness and angle of attack

The difference in height of the zone of influence over the ranges investigated is more than three times greater for a change in relative roughness than for a change in the angle of attack.

Therefore, the hypothesis which stated that the interface's angle of attack has a negligible effect on the height of the zone of influence has been proved false. However, the hypothesis that the effect of the interface height is far more influential than its angle of attack on the behaviour of the soil particles is in fact true.

5.2 Further discussion

5.2.1 Applications

How much soil is being involved in the shearing process is simply not known. The results of this project make progress towards understanding and demonstrating how much soil may actually be involved.

5.2.2 Convection patterns within the array of discs

The experiments in this project have shown a similar behaviour to the convection patterns described by Eshuis *et al.* (2010)[12]. This is particularly noticeable in the PIV vector plots, such the displacement field for interface A2 shown in *Figure 4.1.2*, where the discs appear to map out a circular path.

5.2.3 Circular shape of the photoelastic images

In all of the photoelastic images (*Figure 4.2.1-4.2.5*), there appears to be a curved shaped to the stress field around the edges of the images. The cause of this is the circular lens on the camera which looks at the discs in the centre of the image face-on but observes the discs closer to the edges of the array obliquely. This does not alter the results but it does help to explain the appearance of the images.

5.2.4 Settlement

Movement of particles does occur outside of the zone of influence in the form of settlement. Settlement is seen above the interface in the PIV plots.

5.2.5 Limitations of the experiments

When shearing against a rough interface, a lot of material is initially engaged but the shearing zone soon drops down to close to the bottom of the soil stratum. In the experiments conducted for this project, a single roughness element interface was used. Although this provides useful information about the effect that interfaces of different roughness have on the movement of particles and stresses within the soil, this does not fully simulate a pipe resting on a layer of soil. A pipe is made up of a large number of rough elements, all joined up together.

5.2.6 Dilation

When the soil jams, it is trying to dilate but the soil is resisting this dilation. There is no doubt that the soil is trying to dilate in the experimental setup. The soil was in a packed state initially and so when it shears, it is going to dilate. Dilation would be occurring but the influence of dilation is muted relative to the influence of the interface.

5.2.7 Horizontal motion of particles

In a number of the PIV tests that were run, significant horizontal movement was noted in front of the interface (*Figures 4.1.2, 4.1.3*). This was not seen consistently because the phenomenon is a consequence of the initial packing conditions. Chains of particles form along the bottom of the array and these are moved intact by the interface in the direction of motion.

5.2.8 Extend if the shearing zone

Kuo and Bolton (2014)[23] observed that the shearing zone extended some distance inside the soil; however, once breakout had occurred, the shearing zone tended to coincide with the top of the interface. This phenomenon is not so well observed in the results of this project. This project aims to understand the fundamental behaviour of one interface roughness element rather than a whole series of them.

Chapter 6: Conclusions

6.1 Key results

- The height of the zone of influence is the same for the acrylic and polyurethane arrays
- The height of the zone of influence increases with the relative roughness
- The height of the zone of influence decreases with an increased angle of attack

6.2 Reservations and limitations

There was large scope for human error in this investigation. The main difficulty encountered was determining the exact height of the zone of influence for both the acrylic and polyurethane discs. Engineering judgement was used to read these heights off the PIV vector plots and the photoelastic images and three videos were taken of each test, from which vector plots and photoelastic photos were produced so that an average of the results could be taken and so that anomalies could be identified and removed.

6.3 Implications of the key results

The larger the relative roughness of an interface, the rougher the surface that it simulates. These results therefore suggest that the motion of a rougher surface shearing an array of soil will engage a larger volume of soil than a smoother surface will. The soil resists the motion of the shearing surface with greater participation when the surface is rough than when it is smooth.

Applying these findings to the case of oil pipelines resting on the sea bed, if the pipelines are covered with a rough coating they will feel a greater resistance to motion from the soil beneath them than if they had a smooth coating. A rough coating is therefore desirable.

6.4 Ideas for future work

There are numerous ways in which this work could be extended.

A clear extension of this project would be the quantification of the stresses induced by the shearing rather than simply the location of the stress paths. This would require come sort of calibration, either using the properties of the polyurethane or, more empirically, by testing individual discs using a load cell.

Investigating the effect of interfaces shearing a three-dimensional array could produce interesting results. The use of spheres rather than discs may better simulate the particle interactions. This would involve the use of stereoscopic PIV, as mentioned in section 2.2. Photoelasticity is not commonly used on three-dimensional systems although experiments of this nature at Duke University are currently being undertaken.[9]

An obvious extension would be the inclusion of different phases such as water or a heavy gas to simulate water. Actual soil particles will have a different density and buoyancy to the discs used in this experiment so different discs must be used or a method of accounting for this discrepancy must be designed and implemented. Further investigation could also be undertaken on how the results of this project tie in with fluid mechanics.

If the apparatus could be used upside down, such that the interface runs along the top of the disc array, this may be more applicable to pipelines resting on the seabed because of the reduced residual stress in the grains at the interface.

Perhaps a line of interfaces, which forms a flat gear or line of teeth, would better simulate a rough surface. The superposition of the effect of multiple interfaces could therefore be investigated. This would also make it easier to measure the height of the zone of influence since this zone would have greater lateral extension than for the single interface case.

Acknowledgements

This paper is prepared with the support of Cambridge University Engineering Department University. The author wishes to thank his project supervisor Dr Matthew Kuo for his continued guidance and advice. Special thanks must go to Miss Elizabeth Hepworth for her patience.

References

[1] Ganesan S.A., Kuo M., and Bolton M. (2013), *Influences on Pipeline Interface Friction Measured in Direct Shear Tests*, Geotechnical Testing Journal 37(1), 1-12

[2] Kuo, M.Y-H. (2011), *Deep ocean clay crusts: behaviour and biological origin*, PhD thesis, Cambridge University

[3] Hill, Andy. Senior Geotechnical Engineer, BP Exploration (Personal communication, 20th May 2014)

[4] Behringer B. (2013), *Behringer Group: Research*, http://behringer.phy.duke.edu/pages/research.php, (Accessed 13/01/14)

[5] O'Hern C. S., Silbert L. E., Liu A. J. and Nagel S. R. (2003), *Jamming at zero temperature and zero applied stress: The epitome of disorder*, Phys. Rev. E 68

[6] Torquato S. and Stillinger F.H. (2001), *Multiplicity of generation, selection, and classification procedures for jammed hard-particle packings*, J. Phys. Chem. 105

[7] White D.J. and Take W.A. (2002), *GeoPIV: Particle Image Velocimetry (PIV) software for use in geotechnical testing*, CUED/D-SOILS/TR322

[8] Oliphant J., and Maconochie A. (2007), *The Axial Resistance of Buried Unburied Pipelines*, Proceedings of SUT Offshore Site Investigation and Geotechnics International Conference, London

[9] Behringer B. (2013), *Bob Behringer's Home Page*, http://www.phy.duke.edu/~bob/ (Accessed: 13/01/14)

[10] Zhang J., Majmudar T. S., Sperl M. and Behringer R. P. (2010), *Jamming for a 2D granular material*, Soft Matter 6, 2982-2991

[11] Ovarlez G., Barral Q., Coussot P. (2009), *Three-dimensional jamming and flows of soft glassy materials*, Université Paris Est, Laboratoire Navier, LMSGC (CNRS-ENPC-LCPC)

[12] Eshuis P., van der Meer D., Alam M., van Gerner H. J., van der Weele K., and Lohse D. (2010), *Onset of Convection in Strongly Shaken Granular Matter*, Phys. Rev. Lett. 104

[13] Gerritsen M. (1996), *Particle Image Velocimetry (PIV)*, http://syr.stanford.edu/PIV1.htm (Accessed: 15/05/14)

[14] Kiger K. (2010), *Introduction of Particle Image Velocimetry*, http://www2.cscamm.umd.edu/programs/trb10/presentations/PIV.pdf (Accessed: 15/05/14)

[15] Jahanmiri M. (2011), *Particle Image Velocimetry: Fundamentals and Its Applications*, Research report, Chalmers University of Technology, Sweden

[16] Raffel M. et al. (2007), *Particle Image Velocimetry: A Practical Guide*, 2nd Edition, Springer-Verlag Berlin Heidelberg, Berlin, Germany

[17] Brossard C. et al. (2009), *Principles and Applications of Particle Image Velocimetry*, Aerospace Lab Journal. 1, pp.1-11

[18] Take W.A. (2002), *The influence seasonal moisture cycles on clay slopes*, PhD Dissertation, University of Cambridge

[19] White D.J. (2002), *An investigation into the behaviour of pressed-in piles*, PhD Dissertation, University of Cambridge

[20] Doyle J.F., Phillips J.W. (1978), *Manual on Experimental Stress Analysis*, 5th Edition, Society for Experimental Mechanics

[21] Phillips J.W. (1998), *Experimental Stress Analysis*, Chapter 6, University of Illinois at Urbana-Champaign

[22] Strainoptic Technologies (2010), *Fundamentals of photoelasticity*, http://www.strainoptics.com/files/Fundamentals%20of%20Photoelasticity.pps, Accessed (15/05/14)

[23] Kuo M.Y-H and Bolton M.D. (2014), *Imaging of crushable grains when shearing against rough interfaces*, University of Cambridge

Appendix A: Risk assessment retrospective

The risk assessment, which was conducted before the project began, found that every risk encountered would provide a low or very low residual risk, once the prescribed control measure had been implemented. The main hazards identified in this risk assessment are detailed in *Table A1* below.

Hazard	Effect	Control measures	Residual risk
Worm gear actuator	Items caught in gear	Do not wear loose clothing Do not place fingers close to gear when in operation When operating, gear is fully enclosed	Very low
Tipping of experimental apparatus	Injury to fingers Polyurethane discs falling out	Ensure apparatus is properly secured and supported at base with brackets Stick cling film over top gap to prevent discs falling out	Low
Trip hazard due to dropped polyurethane discs	Slipping on discs	When installing discs into apparatus, install horizontally then move to vertical Use cling film to cover top gap to prevent discs falling out	Low
Cutting out polyurethane discs	Cut fingers	Take due care in positioning fingers away from cutting tool	Low
Cutting out polyurethane discs	Plastic shavings entering eye	Eye protection worn when cutting out discs	Low
Use of paraffin to clean discs	Chemical fumes Skin irritation Disposing of paraffin	Only use in well-ventilated areas Use gloves Discuss with workshop method of disposing of waste paraffin	Low

Table A1: Initial risk assessment

There were very few risks which were encountered during the course of the project, which had not been identified in the initial risk assessment. Two issues which arose were that the edges of the acrylic sheets used to house the discs were sharp and in order to reduce the size of oversized components, given the nature of the bespoke apparatus, filing tools were used. A risk assessment for these additional risks is presented in *Table A2* below.

Hazard	Effect	Control measures	Residual risk
Sharp edges of acrylic	Cut fingers	Smooth off sharp edges with sandpaper or file Use gloves if necessary	Low
Use of tools for filing down oversized components	Shaving in eye	Wear eye protection	Low

Table A2: Risk assessment of additional risks

Were the project to be repeated, there would be no alterations to the original risk assessment other than those presented in *Table A2.*